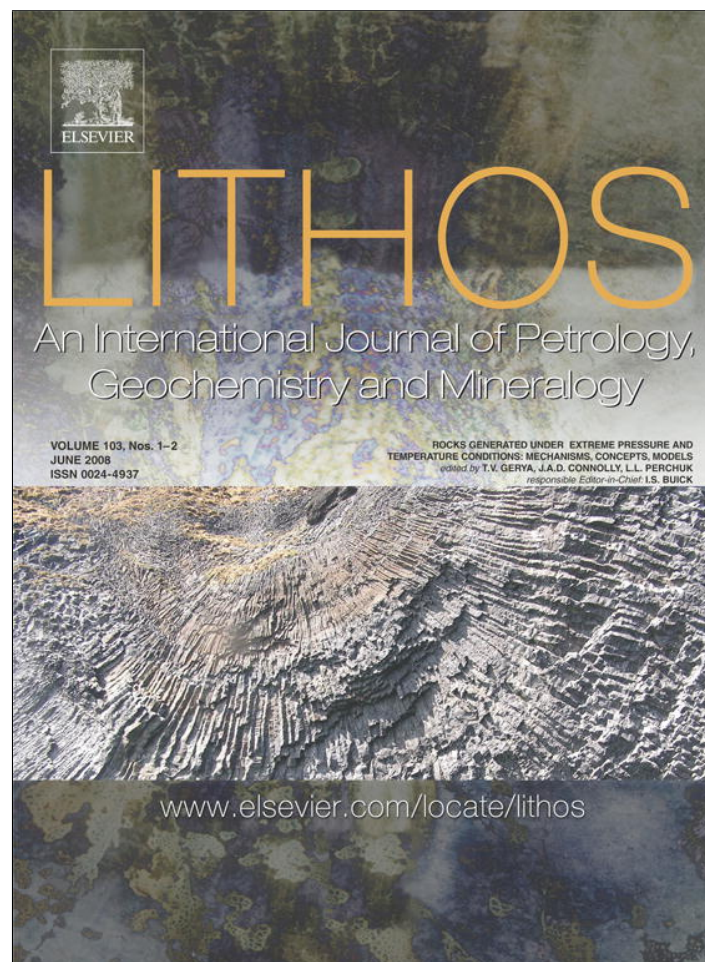


Provided for non-commercial research and education use.
Not for reproduction, distribution or commercial use.



This article appeared in a journal published by Elsevier. The attached copy is furnished to the author for internal non-commercial research and education use, including for instruction at the authors institution and sharing with colleagues.

Other uses, including reproduction and distribution, or selling or licensing copies, or posting to personal, institutional or third party websites are prohibited.

In most cases authors are permitted to post their version of the article (e.g. in Word or Tex form) to their personal website or institutional repository. Authors requiring further information regarding Elsevier's archiving and manuscript policies are encouraged to visit:

<http://www.elsevier.com/copyright>



Continental plate collision, P – T – t – z conditions and unstable vs. stable plate dynamics: Insights from thermo-mechanical modelling

Evgenie Burov*, Philippe Yamato

Lab Tectonique UMR 7072, University of Pierre and Marie Curie, 4 place Jussieu, 75252 Paris, France

Received 4 May 2006; accepted 3 September 2007

Available online 3 October 2007

Abstract

There was much debate recently on the mechanisms of continental convergence and related pressure–temperature (P – T) conditions, both in modeling and petrologic community. Depending on the mechanisms of convergence (subduction, collision, folding or RT instability) one can argue about the possibility of large-scale deviations of pressure and temperature in the accretion prism and below it, from “reference” (i.e. lithostatic) conditions commonly used for petrologic reconstructions of evolution of exhumed metamorphic rocks. These deviations can be caused, for example, by tectonic overpressure that, as suggested in some studies, may be responsible for formation of UHP (Ultra High Pressure) rocks. However, overpressure in exhumation zones can be built only in specific collision scenarios associated with plate coupling (pure shear, folding). In this study, we analyze conditions that define various mechanisms of convergence, and consequently, of exhumation. These mechanisms can be represented as a superposition of (1) simple shear (subduction), (2) pure shear (collision), (3) folding and (4) Rayleigh–Taylor instability. We study these scenarios using a thermo-mechanical model that accounts for brittle–elastic–ductile rheology, surface processes, and metamorphic changes. It appears that stable, “oceanic-type” subduction may occur in the case of cold lithospheres ($T_{\text{Moho}} < 550$ °C) and relatively high convergence rates (> 3 – 5 cm/yr). Depending on the lower-crustal rheology (strong or weak), either the whole (upper and lower) crust or only the lower crust can be involved in subduction. In case of weak metamorphic rheologies, phase changes improve chances for stable subduction. Pure shear becomes a dominant mechanism when $T_{\text{Moho}} > 550$ °C or convergence rates are lower than 3 cm/yr. Large-scale folding is favored in case of $T_{\text{Moho}} = 500$ – 650 °C and is more effective in the case of mechanical coupling between crust and mantle (e.g., strong lower crust). Gravitational (Rayleigh–Taylor) instabilities overcome other mechanisms for very high values of $T_{\text{Moho}} (> 800$ °C) and may lead to development of subvertical “cold spots.” However, it is reasonable to assume that in most cases continental collision is initiated at oceanic subduction rate, which is rarely slower than 5 cm/yr. This rate is sufficient to drive continental subduction during the first several Myr of collision. In this case, the subduction channel is characterized by nearly lithostatic pressure conditions. Large-scale zones of tectonic overpressure may be built outside the channel but do not affect the exhumed rocks. Overpressure may be built inside the channel in the short moment of its closure. We suggest that most continental orogenic belts could have started their formation from continental subduction. This evokes small tectonic overpressures and thus deep origin of the UHP rocks that may be brought to the surface via the suggested multi-level mechanism of exhumation.

© 2007 Elsevier B.V. All rights reserved.

Keywords: Continental collision; Orogens; Exhumation; Metamorphism; Modeling; Rheology

* Corresponding author.

E-mail address: evgenii.burov@lgs.jussieu.fr (E. Burov).

1. Introduction

1.1. Pressure in convergence zones: lithostatic or non-lithostatic?

Pressure and the state of stress in the continental lithosphere have been a topic of long debate since the emergence of the gravity potential theory (e.g., Artyushkov, 1973; Dahlen, 1981; Fleitout and Froidevaux, 1982, 1983; England and Houseman, 1989). According to estimates made from isostatic and also large-scale mechanical stress models (e.g., Cloetingh et al., 1982), gravity driven plate tectonic forces should not exceed 10^{12} – 10^{13} N. This yields average deviatoric intraplate stresses on the level of 10–100 MPa, i.e. small compared to the pressure of High Pressure (HP) or Ultra High Pressure (UHP) metamorphism recorded in collision zones (2–3 GPa). These estimates have lead most workers to the conclusion that pressure conditions in the lithosphere are not significantly different from its gravitational (lithostatic) component ρgz (where ρ is the density, g is the acceleration due to gravity, z is the depth). The assumption of a lithostatic pressure gradient has allowed for simple decoding of petrological data in terms of depth and thus for putting forward a number of hypotheses on the mechanisms of exhumation and collision, among them the well known model of the critical accretion wedge (corner flow) (e.g., Dahlen, 1981; Platt, 1986, 1993). Yet, it was argued later (Mancktelow, 1995; Petrini and Podladchikov, 2000) that the pressures recorded by metamorphic rocks do not automatically reflect the depth of their formation, since the recorded pressure can be higher or lower than the lithostatic level. Indeed, complete pressure P is:

$$P = 1/3 \sigma_{ij} \delta_{ij} \quad (1)$$

where σ_{ij} corresponds to the components of the stress tensor, δ is Kroneker delta, equal unity if $i=j$, 0 otherwise. P thus equals mean normal or principal stress that may be different from ρgz . In convergence settings associated with important pure shear deformation, P can be built up over the lithostatic pressure ρgz in stiff zones of the lithosphere, until the differential stress reaches the yielding limit (Petrini and Podladchikov, 2000). In brittle materials, yielding stress increases with pressure, so a rheological feedback can be established and total pressure will grow with compression or decrease with extension. Petrini and Podladchikov (2000) made the following simple analysis:

$$P = 1/3(\sigma_{11} + \sigma_{22} + \sigma_{33}) \approx 1/3(\sigma_1 + P + \sigma_3) \quad (2)$$

hence $P \approx 1/2(\sigma_1 + \sigma_3)$

assuming a Mohr–Coulomb rheology with a frictional angle ϕ , zero cohesion (Byerlee's law) and a pore pressure factor a , one obtains for compression ($\sigma_3 \approx \rho gz$) from the relation $1/2(\sigma_1 + \sigma_3) \sin \phi = 1/2(\sigma_1 - \sigma_3) = 1/2 \Delta \sigma$:

$$P \approx \rho gz(a \sin \phi - 1)/(\sin \phi - 1) \quad (3a)$$

Assuming $\phi \approx 30^\circ$ and $a=0$ (dry rock):

$$P \approx 2\rho gz \quad (3b)$$

This means that in compressional environments, total pressure may be twice lithostatic, if the material is found in total yield state that may be reached in pure shear deformation mode (collision, folding). In simple shear (subduction), however, the total pressure depends on the degree of coupling (i.e. degree of transmission of horizontal stress) between the upper and lower plate. If the lower plate sinks by its own, the total pressure would be close to ρgz . Pressure deviations from the lithostatic level can be also obtained in viscous (dynamic pressure), elastic or visco-elastic rock. For example, ductile flow builds dynamic pressure p (Table 1),

$$P \approx \rho gz + p \text{ where } p = \frac{1}{2} \left(\frac{\dot{\epsilon}}{A} \right)^{\frac{1}{n}} \exp \left(\frac{Q}{nRT} \right) \quad (4)$$

In elastic rock, pressure is limited only by the amount of strain and by the value of shear modulus.

Based on these considerations, Petrini and Podladchikov (2000) have suggested that tectonic overpressure may boost total pressure to $1.6\rho gz - 2\rho gz$. This proposition implies reduction by a factor of 1.6–2 of the possible depth of UHP exhumation (60 km instead of 120 km, 75 km instead of 150 km, and so on), and makes the application of common shallow exhumation models such as the accretion wedge model possible. Earlier, Mancktelow (1995, Fig. 1b model D) has suggested that dynamic pressure p in the subduction channel may be as high as ρgz and thus the total pressure as high as $2\rho gz$.

1.2. Subduction and pressure–temperature conditions

As follows from the above discussion, the pressure and stress state in the exhumation zones depends on the mechanism of accommodation of convergence (pure shear, simple shear, folding etc) and on the physical and rheological properties of the rocks (strong or weak subduction channel, upper–lower plate coupling–uncoupling, crustal delamination etc.). For example, Petrini and Podladchikov's (2000) overpressure model relies on the applicability of the Byerlee's law (Byerlee, 1978) of brittle failure at 40–60 km depth. However, doubts exist

Table 1
Summary of thermal and mechanical parameters used in model calculations

Thermal	Surface temperature (0 km depth)	0 °C
	Temperature at the base of thermal lithosphere	1330 °C
	Temperature at the base of upper mantle (650 km)	2000°±100 °C
	Thermal conductivity of crust	2.5 W m ⁻¹ °C ⁻¹
	Thermal conductivity of mantle	3.5 W m ⁻¹ °C ⁻¹
	Thermal diffusivity of mantle	10 ⁻⁶ m ² ·s ⁻¹
	Radiogenic heat production at surface	9.5×10 ⁻¹⁰ W kg ⁻¹
	Radiogenic heat production decay depth constant	10 km
	Thermo-tectonic age of the lithosphere	50 to 600 Myr
	Mechanical	Density of the upper crust
Density of lower crust		2900 kg m ⁻³
Density of oceanic crust		2900 kg m ⁻³
Density of sediment		2600 kg m ⁻³
Density of mantle		3330 kg m ⁻³
Density of asthenosphere		3310 kg m ⁻³
Lamé elastic constants λ , G (Here, $\lambda=G$)		30 GPa
Byerlee's law–Friction angle		30°
Byerlee's law–Cohesion		20 MPa

in the applicability of this law below 30 km depth (e.g., Kirby et al., 1991). Starting from this depth, weak semi-brittle behaviours or plasticity mechanisms such as Piers plasticity (Goetze and Evans, 1979) may limit brittle strength to 0.5–0.7 GPa (Ranalli, 1995). If true, it is impossible to reach a total pressure of 2 GPa at depths of 30–60 km, whereas the UHP rocks form at $P=3$ GPa and temperatures, indicating sub-Moho depths (>700–800 °C). Unfortunately, temperature–depth relations in collision zones are quite uncertain so that temperature cannot be easily decoded in terms of depth, and thus serve as an additional constraint on the inferred pressure–depth dependencies. Stable shear heating, for example, may be responsible for 100–200 °C increase of temperature in subduction channel, whereas co-seismic heating may even result in partial melting (Turcotte and Schubert, 2002; Gerya et al., 2008). On the other hand, if one forgets the shear heating, temperature in the subduction channel must be “colder” than in the normal lithosphere at the same depth, due to the permanent advection of cold rock from the surface. Depending on the advection (=subduction) rate, temperature in the subduction channel may be 100–500 °C lower than in the normal lithosphere. This cold thermal gradient is actually needed to preserve ductile strength and thus integrity of the subducting plate until its crustal part reaches the UHP depth, otherwise weakened ductile crustal material would detach from the mantle lithosphere at shallower depth. Accounting both for shear heating and advection, temperatures are unlikely to reach 800 °C in the subduction channel above 40 km depth (normal Moho depth). Formation of HP eclogites

requires temperatures exceeding $T=500$ °C. In normal continental settings, such temperature is predicted for 40 km depth, but should be found twice or three times deeper inside the subduction channel. At $T>500$ °C, most crustal rocks are ductile, have a low strength and cannot be significantly over-pressured. Finally, it should be not also forgotten that the temperature distribution inside the subduction channel depends on the initial temperature of the crustal material advected from the surface. This temperature is affected by the dynamics of the accretion wedge that is both cooled due to filling by cold sedimentary material and heated due to the accumulation of radiogenic heat sources and thermal blanketing (Stephenson et al., 1989; Lavier and Steckler, 1997).

As mentioned above, subduction of any lithosphere (oceanic or continental) requires that the plate remains cold enough to partly preserve its initial strength as it sinks into the asthenosphere. Otherwise the plate will break-off, thicken, or drip-off due to viscous gravitational (Rayleigh–Taylor) instabilities. The subduction is equivalent to a condition that the intraplate strain rate is small so that the plate-parallel component of velocity of the plate remains nearly constant along its length. Since the slab push and pull forces acting on the opposite ends of the plate are largely different, this can be only observed if the slab stays strong at depth, i.e. has no time to heat up and weaken due to the influx of heat from the surrounding hot (1330 °C) asthenosphere. One can characterize this minimal condition for stable subduction by the Péclet number Pe :

$$Pe = u_x^2 t / \kappa \quad (5)$$

where t is a characteristic time scale, u_x is plate-parallel (horizontal at surface) plate velocity and κ is thermal diffusivity (\approx on the order of $10^{-6} \text{ m}^2 \text{ s}^{-1}$). The corresponding thermal diffusion length is then $l_d = (t \kappa Pe)^{1/2}$.

For preservation of slab strength, l_d should be significantly less than h_k , where h_k is the minimal thickness of the strong “elastic” core preserved within the slab.

This core is needed for transmission of in-plane stresses without breaking or thickening the lithosphere.

$$Pe > Pe_k \text{ where } Pe_k = u_x h_k / \kappa \quad (6)$$

If Pe is smaller than Pe_k , thermal weakening prohibits a stable subduction process. Observations of plate flexure reveal significant plate strength in zones of oceanic

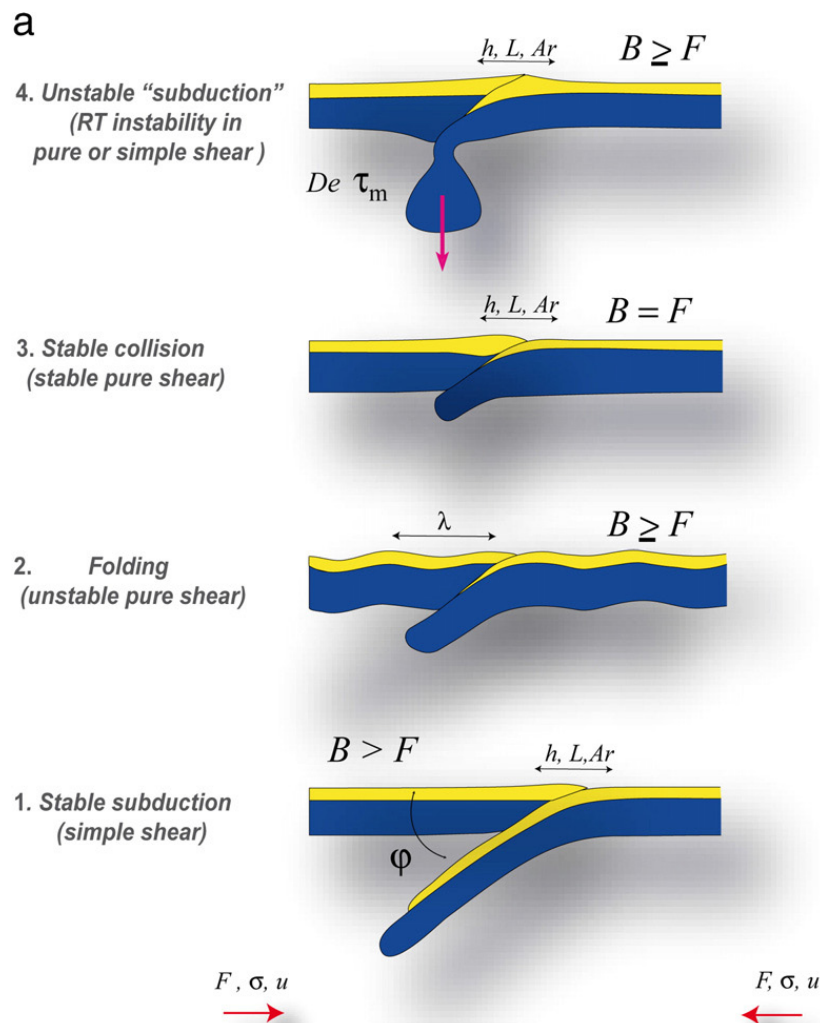


Fig. 1. a. Possible collision scenarios: simple shear in stable mode (subduction, 1), pure shear in unstable (folding, 2) and stable mode (3), unstable pure or simple shear (Rayleigh–Taylor instability, 4). Related large-scale parameters characterising collision style, lithospheric strength and rheology: T_e , F , σ , u , De , τ_m , h , L , λ , ϕ . T_e is equivalent elastic thickness. F , σ , u are respectively the horizontal force, stress and convergence/extension velocity, that are linked to the lithospheric strength and possible deformation styles. De and τ_m are respectively Deborah number and relaxation time related to viscosity contrasts in the lithosphere. λ is the characteristic wavelength of unstable deformation related to the thickness of the competent layers in the lithosphere. h , L are respectively the vertical and horizontal scale for process-induced topography supported by lithospheric strength, Argand number $Ar = \rho g h L / F$. ϕ is subduction or major thrust fault angle that is indicative of the brittle properties and of the overall plate strength. b. Various exhumation models associated with different continental subduction and collision mechanisms: (A) classical accretion prism mechanisms for LP–LT to MP–MT conditions (Davis et al., 1983; Dahlen and Suppe, 1988; Dahlen, 1990); (B) Thrusting model, superimposed here onto accretion prism mechanism (LP–LT to MP–MT conditions, e.g., Jolivet et al., 1994); (C) Thompson’s et al. (1997) “toothpaste squeezing” high-rate exhumation model; (D) Mancktelow’s (1995) “rocket nozzle” dynamic overpressure model (LP to UHP conditions, Mancktelow, 1995); (E) pure shear overpressure model (Petrini and Podladchikov, 2000); (F) megabuckling overpressure and exhumation model for Himalayan syntaxes (Burg and Podladchikov, 2000); (G) rigid block UHP exhumation model (Chemenda et al., 1995); (H) and (I) multi-stage soft crust exhumation model (LP to UHP conditions, high or low degree of metamorphism, or high or low density of the metamorphic grades, Burov et al., 2001) that may be combined with the hot channel mechanism suggested by T. Gerya (Gerya et al., 2008).

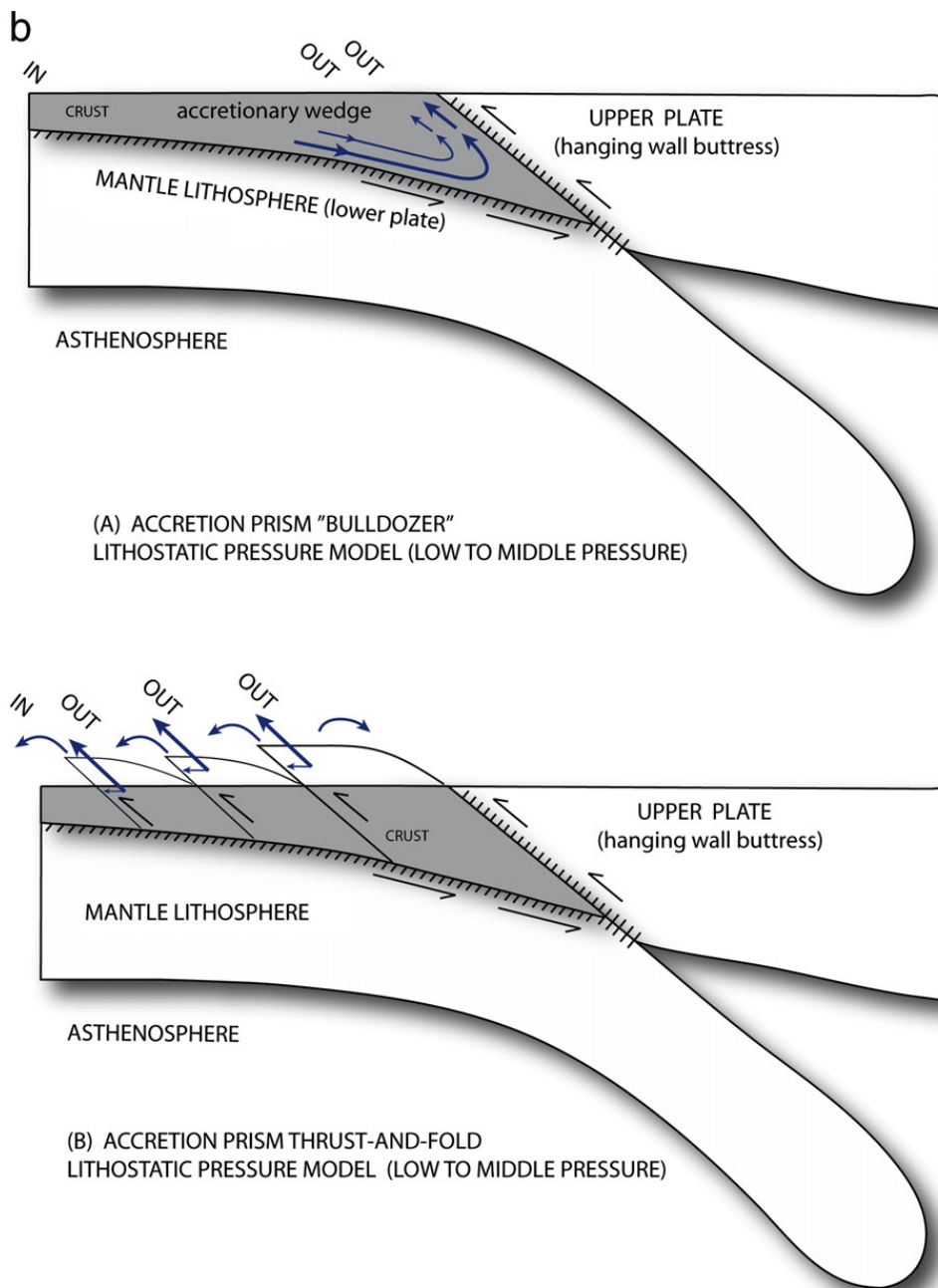
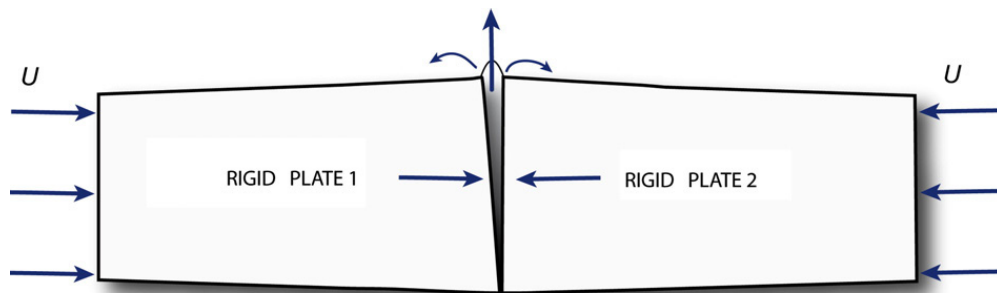


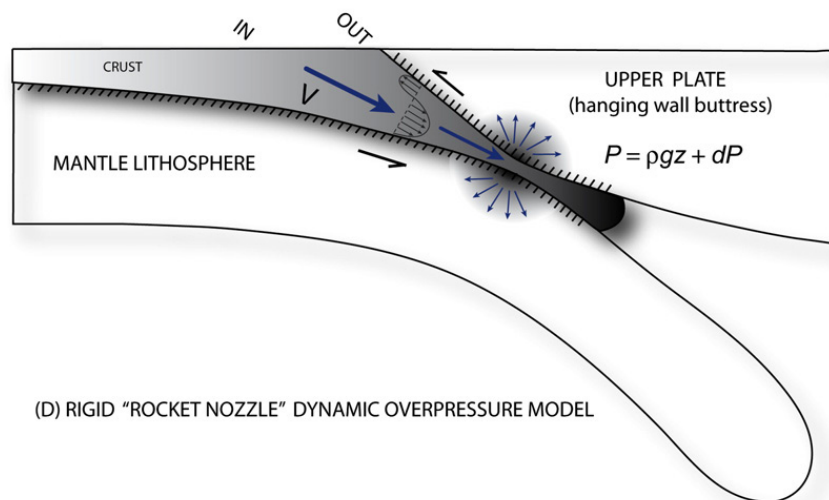
Fig. 1 (continued).

subduction. A typical value of the Equivalent Elastic Thickness (EET) of the oceanic lithosphere, which is roughly determined by the depth to the 600 °C geotherm, is 30–50 km (e.g., Burov and Diament, 1995). By analogy with the oceanic plates, which, as we know, do subduct, we can assume same minimal EET value for subducting continental lithospheres. Continental plates are characterized by EET values varying between 15 and 90 km (e.g., Burov and Diament, 1995; Cloetingh and Burov, 1996; Burov and Molnar, 1998; Pérez-Gussinyé and Watts,

2005). Some of them thus should be strong enough to develop oceanic-type subduction provided that other conditions (e.g., buoyancy versus shear force balance) are also favorable. For example, consider a convergence rate u_x of 1 cm/y. Assuming a value for h_k of 50 km we obtain $Pe_k=15$. For t on the order of a few Myr, Pe is smaller than Pe_k , suggesting that subduction is improbable at such a slow convergence rate. However, for $u_x=5$ cm/y, $Pe_k=75$ and $Pe=400$ suggesting that stable subduction is not prohibited in this case.



(C) "TOOTH PASTE" "SQUEEZING" EXHUMATION MODEL

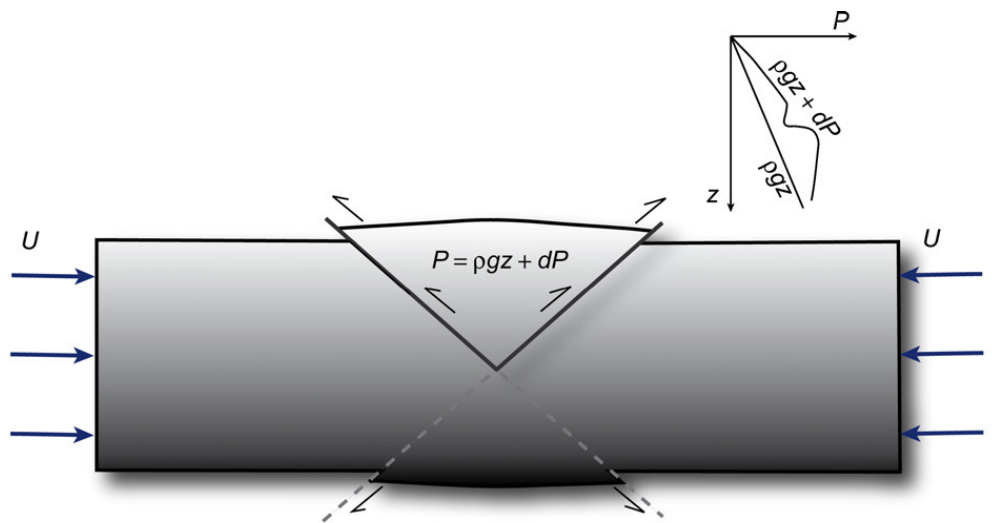


(D) RIGID "ROCKET NOZZLE" DYNAMIC OVERPRESSURE MODEL

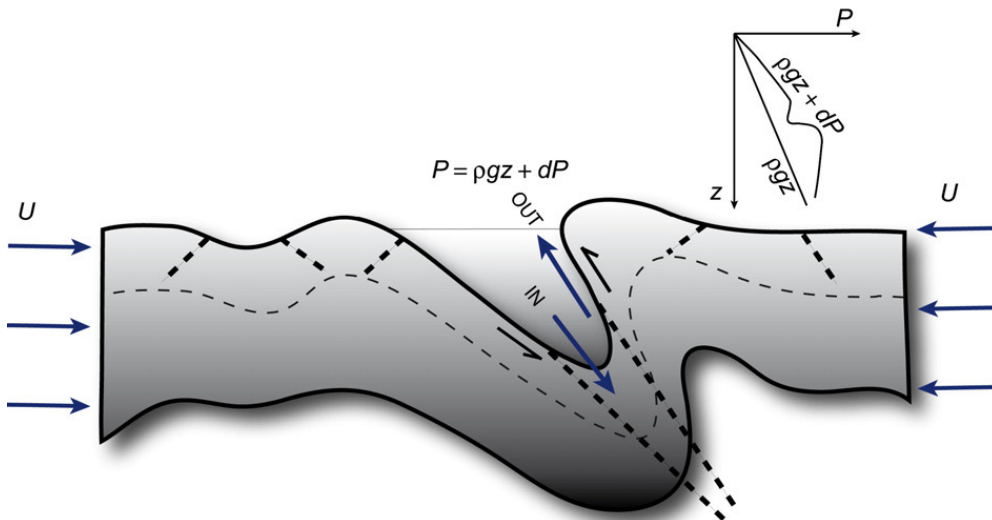
Fig. 1 (continued).

In nature, many additional conditions must be satisfied to allow for development of continental subduction. In particular, growth rates of the competing modes of deformation (RT instability, folding, pure shear) should be small, and the upward drag due to the buoyant crust and viscous shear must be smaller than tectonic and slab pull forces. The combined effect of these multiple factors was recently assessed from numerical modeling (Toussaint et al., 2004a,b; Burov and Watts, 2006). These parametric studies have shown that continental subduction can occur and remain sustained over tens of million years if the continental lithosphere is initially cold, with a temperature at the Moho depth less than 550 °C, and if the convergence rate is higher than 3–4–5 cm/yr. It is therefore reasonable to assume that after the onset of the collision between, for example, India and Eurasia, when the convergence rate was about 10 cm/y, (Patriat and Achache, 1984), the oceanic subduction could be followed by subduction of the Indian lithosphere (Toussaint et al., 2004b).

Despite these complexities, a number of geologic and geophysical observations point to the possibility of stable continental subduction (e.g., Chopin, 1984). Yet, this requires additional explanatory models. For example, the problems related to the positive buoyancy of the lithosphere can be circumvented if the light crust early separates from the mantle (Cloos, 1993) or if it undergoes metamorphic changes and becomes dense and strong (Austheim, 1991; Le Pichon et al., 1992; Burov et al., 2001). Geodynamic data also suggest that during the first millions years of transition from ocean–continent subduction to continent–continent collision, the convergence rates are considerably higher than at later stages. For example, in case of India–Asia collision, the convergence rate has slowed down from the initial 10–15 cm/y during the first 10–15 Myr to less than 5 cm/y at present (Patriat and Achache, 1984). The elevated early convergence rates favor the initial development of continental subduction that may be followed by a different deformation mode (pure shear, folding, etc.) as the convergence rate slows down.



(E) PURE SHEAR OVERPRESSURE MODEL



(F) MEGABUCKLING (UNSTABLE PURE SHEAR) EXHUMATION MODEL WITH OVERPRESSURE

Fig. 1 (continued).

One can summarize the different mechanisms of accommodation of lithospheric shortening as follows (Fig. 1a): (1) pure-shear thickening; (2) simple shear subduction or underplating; (3) folding (Cloetingh et al., 1999; Burg and Podladchikov, 2000), and (4) gravitational (Rayleigh–Taylor (RT)) instabilities in thickened, negatively buoyant lithosphere. The RT instabilities lead to sinking of subvertical sections of lithosphere into the asthenosphere (e.g., Houseman and Molnar, 1997), which we dub “unstable subduction.” Superimposed scenarios are also possible: for instance, “megabuckles” created by lithospheric folding (Burg and Podladchikov, 2000) can localize and evolve into subduction-like zones or result in the development of Rayleigh–Taylor instabilities. On the

other hand, RT instabilities can also occur in subducting lithosphere (Pysklywec et al., 2000).

1.3. Exhumation models

The mechanisms of exhumation of HP and UHP rocks constitute a major geodynamic problem closely related to the problem of P – T – t – z relations in collision settings. These high density rocks (e.g. eclogite density may exceed by 100 kg/m^3 that of the mantle (3330 kg/m^3)) are particularly difficult to exhume to the surface by the conventional exhumation models developed for LP and MP exhumation. The suggested models can be roughly sub-divided in shallow kinematically driven exhumation

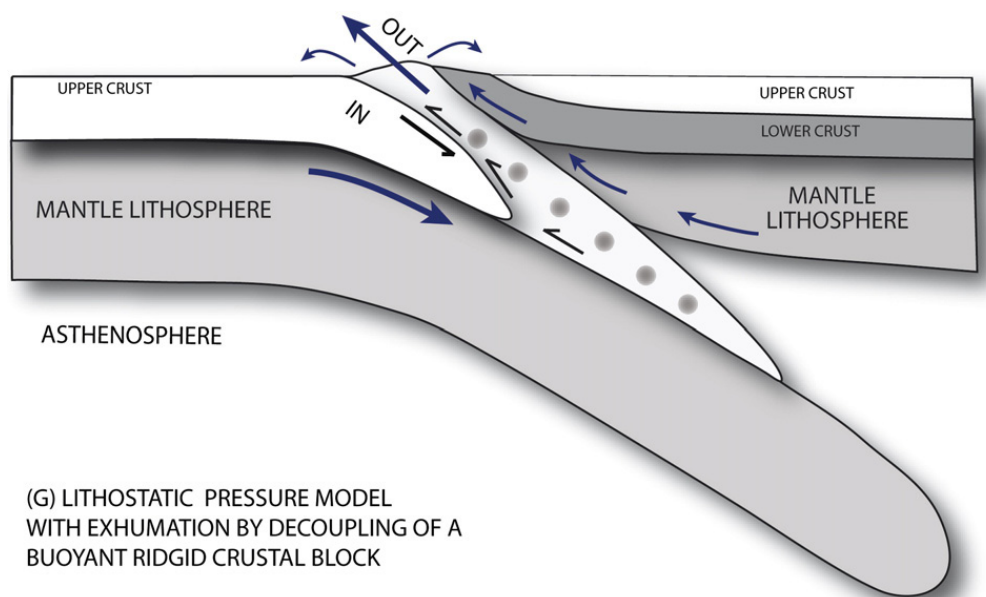


Fig. 1 (continued).

models with overpressure and deep basically hydrodynamically driven exhumation models with nearly lithostatic pressure.

If one accepts lithostatic pressure conditions for subduction channel settings, then the exhumation depth of HP and UHP rocks must exceed 80–120 km. It was demonstrated (e.g., Platt, 1993, Fig. 1b model A) that the most common exhumation mechanism that refers to kinematically forced circulation in the critical wedge of an accretional prism (Davis et al., 1983; Dahlen and Suppe, 1988; Dahlen, 1990) cannot bring metamorphic material to the surface from depths exceeding 40 km. This limitation is related to the fact that the accretion wedge mechanism requires, at one side, a relatively high viscosity, needed to drag host rocks to depth and bring their metamorphic facies back to the surface, but on the other side, the viscosity cannot be higher than 10^{19} Pa s to permit circulation of matter and maintain a realistic geometry of the sedimentary prism (Emerman and Turcotte, 1983). At temperatures corresponding to the 40 km depth, most metamorphic rocks have a low viscosity and it becomes impossible to build a sufficiently high viscous force to drag such a weak material up. As a result, some part of the material will remain at the bottom of the accretion prism or will be carried down with the subducting mantle. Another classical kinematic exhumation model evokes foreland fold-and-thrust mechanisms (Fig. 1b case D) allowing to thrust one rock unit on top of another. Thrusting coupled with erosion may bring up rocks only from crustal depths and thus also cannot ex-

plain HP and UHP exhumation. It is due to the limitations of the conventional models that Mancktelow (1995, Fig. 1B) and Petrini and Podladchikov (2000, Fig. 1E) have suggested that HP and UHP rocks are formed at shallow depths as a result of tectonic overpressure.

Both overpressure models, Petrini and Podladchikov's (2000, Fig. 1b model E) and Mancktelow's (1995, Fig. 1b, model D) require specific conditions. The first model needs full plate coupling to build up pressure in the exhumation zone. It is not compatible with a subduction scenario where the lower plate "escapes" from collision with the upper plate. In case of subduction, transfer of horizontal stress between the plates depends on the degree of intra-plate coupling. In the oceans, for example, the lower plate is negatively buoyant when it arrives at the subduction zone. It may sink without any "help" from the overriding plate. The overpressure in such a plate is limited to stresses caused by viscous resistance of the asthenosphere to subduction, and thus depends on the subduction rate u , and on the amount of subduction and asthenospheric viscosity.

For the case of weak inter-plate coupling, Mancktelow (1995, Fig. 1b model D) has suggested a dynamic overpressure model where overpressure builds up in progressively narrowing subduction channel. This model works under the assumption that channel walls are rigid and undeformable, and implies Bernoulli's physics for the inverse dependence of flow pressure on channel cross-section, like if it was a high-pressure nozzle. It was later found (Burov et al., 2001), however, that finite mechanical resistance of

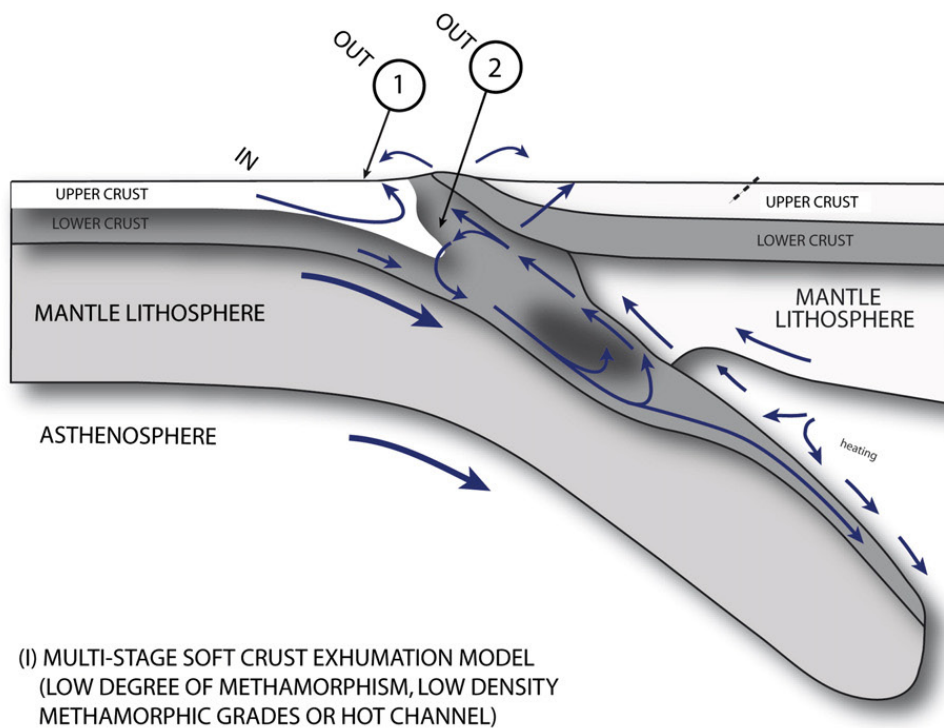
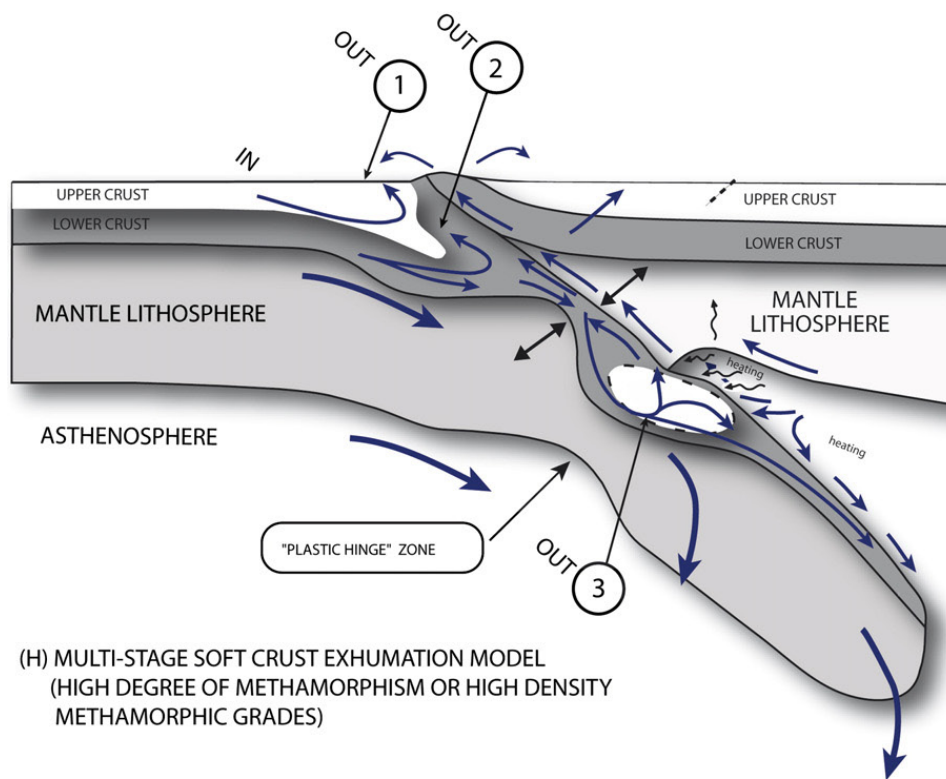


Fig. 1 (continued).

the channel walls does not allow for building of a significant overpressure, since increase of dynamic pressure automatically results in widening of the channel, and, consequently, in restoration of the initial pressure level. In the three-dimensional nature, a pressure rise in the sub-

duction channel would also result in lateral (out of plane) escape of weak material resulting in equilibration of pressure to lithostatic level.

Several other models (Jolivet et al., 1994, Fig. 1b model B; Thompson et al., 1997, Fig. 1b, model C)

attempted to explain exhumation of metamorphic rocks by different mechanisms. For example, Thompson's "tooth paste" model (e.g., Thompson et al., 1997, Fig. 1b model C) suggests that rocks may be squeezed up to the surface, for example as a result of closure of the accretion prism. The model of Thompson et al. (1997) is conceptual; it was not tested by fully coupled thermo-mechanical models. One can suspect that this model requires quite specific rheological properties for the colliding blocks. The kinematic thrust- and-fold models (Jolivet et al., 1994) exploit the possibility of detachment at the base of the accretion prism. In this case the lower accreted units may be folded and thrust on top of the upper units. This model appears to be consistent with many field observations but refers to LP and MP conditions.

Chemenda et al. (1995, Fig. 1b, model G) have suggested a highly elaborated analogue model of a collision–subduction scenario with a lithostatic UHP mechanism, in which the rigid cold crust is initially brought down with the subducting mantle because its initial viscosity is high allowing for its adherence to the subducting mantle lithosphere. Partly metamorphosed but still buoyant and sufficiently rigid crustal blocks return to the surface when they delaminate from the mantle. The delamination is caused by reduction of the ductile strength of the crust as its temperature increases with depth. The heavy UHP units are brought to the surface in solid state with the buoyant low density matrix. Once at the surface, the matrix is eroded exposing less erodible UHP material. As can be seen, the key point of this model relates to the net floatability of the exhumed crustal blocks that are supposed to be only partly converted into metamorphic material. The model of Chemenda has been successfully tested mechanically. This model requires, however, additional validation in terms of the P – T conditions because, as most analogue models, it is not thermally coupled and its P – T conditions are out of control. In particular, one needs to demonstrate that the crustal blocks can remain sufficiently rigid at the moment of their decoupling from the mantle. It should be also kept in mind that phase transitions also may result in reduction of the ductile strength and also depend on the presence of fluids, which remain a poorly constrained factor of the subduction process. With these reservations, one can suggest that the "rigid block model" may work in particular settings characterized by exhumation of small volumes of UHP rock.

In some collision settings such as the Western Alps (e.g., Agard et al., 2001), the amounts of exhumed UHP material are extremely important (large volumes up to 50 km wide). This material is also strongly deformed by ductile deformation. This excludes the possibility that these units were exhumed as small inclusions within a

rigid matrix. For this reason, Burov et al. (2001, Fig. 1b model H, I) have suggested an alternative thermally-coupled numerical model, in which the subduction channel breaks into a shallow (1) and mid-depth (2) accretion wedge and (3) a deep zone of accumulated crustal material formed near the base of the upper plate (this zone is dubbed "crustal pocket"). For each of these three levels there is a specific mechanism of exhumation. The two accretion wedge zones exhume LP and MP pressure rocks and also HP and UHP rocks that penetrate in the prism with return flow in the subduction channel. This return flow is driven both by up-thrusting of the upper plate and small-scale convective movement in the subducted crust and "crustal pocket" at 50–120 km depth. At this depth, the weakened subduction channel breaks down onto two parts, the upper and the lower one (i.e., "crustal pocket"), separated from each other by a more or less narrow neck. Starting from this depth, a large part of the upper and adjacent lower crustal material does not subduct anymore, this material is accumulated below the upper plate and heats up due to direct contact with hot ($T=1330^{\circ}$) asthenosphere. Thermal expansion due to heating starts small-scale convection in the "crustal pocket". This convection drives the metamorphic material back to the intermediate crustal depths (40–50 km). From these depths, the UHP material can be exhumed to the surface in the "normal way", by the accretion prism mechanism. Each stage of exhumation (convective, lower prism and upper prism) has its characteristic exhumation rate. The exhumation rate characterizing the convection stage may be slower but basically much more rapid (10–15 cm/yr) than the tectonic convergence and uplift rates because the ascent (Stokes) velocity is primarily conditioned by the density contrast and viscosity. Burov et al. (2001) suggest that this mechanism can work for a limited amount of time during the initial stages of continental subduction.

Recent numerically inspired UHP exhumation models by Gerya and Stöckhert (2005) and Stöckhert and Gerya (2005) suggested additional exhumation mechanisms, such as Rayleigh–Taylor instabilities in the subduction channel, for oceanic subduction. Similar processes may probably occur in the continents: Rayleigh–Taylor instabilities may develop in the subduction channel due to hydration and partial melting and propel low density "cold plumes" ascending towards the surface (Gerya and Yuen, 2003); back-arc or back-stop exhumation may be partly explained by the formation of rotating rigid "wheels" trapped into the weakened material in the subduction channel (Gorczyk et al., 2006).

The "hot channel" model (Gerya et al., 2008) of continental collision complements the multi-stage model of Burov et al. (2001) by including a new additional

heating–weakening mechanism, in which the subducting crustal material may be over-heated by several sources such as viscous shear heating and radiogenic elements brought to depth with sediments. In this model, heating is also associated with flow of aqueous fluids relieved by rapid dehydration (deserpentinization) of the overriding mantle lithosphere that has been hydrated during previous subduction stages. The channel can penetrate along the plate interface down to the bottom of the lithosphere of the overriding plate (150–200 km) and is characterized by metamorphic temperatures reaching 700 to 900 °C. The low effective viscosity of rocks caused by increased temperature, partial melting and fluid infiltration permits profound mixing of hydrated mantle and crustal rocks. The hot channel exists during the early stage of collision only, but rapidly produces large amounts of ultrahigh-pressure, high temperature rocks. Further collision closes the channel through squeezing rheologically weak, partially molten, buoyant rocks between the strong lithospheric mantles of the two colliding plates.

The specific features of the Burov et al. (2001) and (Gerya et al., 2008; Burg and Gerya, 2005) models refer to the proposition of several stages, or levels, of exhumation, with different exhumation rates at each stage/level. These models predict high exhumation rates at depth that may be several times higher than the horizontal convergence rate or denudation rate at the surface. The predicted rates reach, for example, 10–15 cm/yr in the Alpine context where the average convergence rates are less than 1 cm/y and even the initial convergence rates were unlikely to be higher than 3–5 cm/yr (Burov et al., 2001; Yamato et al., 2007a,b).

Finally, Burg and Podladchikov (2000, Fig. 1b model G) have suggested a specific exhumation model that implies megabuckling of mechanically coupled strong colliding plates. In this model, there is no upper and lower plate but the crustal rocks are brought down within a gigantic anti-cline formed as a result of a compressional instability. These rocks are then exhumed to the surface by denudation processes and possibly by squeezing like in Thompson's model. The possibility of megabuckling or, more general, of “symmetric” collision, was also discussed in Burov et al. (1990) and Cloetingh et al. (1999). However, this kind of scenario might be limited to quite specific places in the world such as Himalayan syntaxes or Tien–Shan.

1.4. Collision–subduction models and their drawbacks

The multitude of factors influencing continental collision justifies a modeling approach (e.g., Chemenda

et al., 1995; Pysklywec et al., 2000; Doin and Henry, 2001; Gerya et al., 2002; Sobouti and Arkani-Hamed, 2002). However, not all existing models are satisfactory. The analogue models are imperfect because of rheological simplifications, poorly controlled thermal coupling and because of the practical impossibility of reproduction of phase changes. The numerical models are often limited by simplified visco-plastic rheologies (e.g., Pysklywec et al., 2000) or by the rigid top upper-boundary condition, that is often used instead of natural free-surface boundary condition. The use of a fixed upper-boundary condition forces stable subduction (Doin and Henry, 2001; Sobouti and Arkani-Hamed, 2002), attenuates pure shear, cancels folding and does not allow for consistent prediction of topography evolution. Many studies simply force a specific convergence mode, for example, subduction, via prescription of strongly favoring boundary conditions, which is sometimes done in physically questionable way by putting an additional boundary condition (e.g., “S-point”) inside the model (e.g., Beaumont et al., 1996; Beaumont et al., 2000). Some other models favor pure shear collision by including a weak zone in the plate shortened in the direction opposite to the pre-imposed mantle flow (Pysklywec et al., 2002).

Consequently, it is important to implement new type of models, which (1) allow for all modes of deformation and (2) account for realistic rheology and thermal evolution. The goal of this paper is to study various factors controlling continental collision and P – T conditions by using most adequate thermo-mechanical models. For that, we suggest a model that combines (1) a free surface boundary condition and surface processes (true topography); (2) realistic brittle–elastic–ductile constitutive model and structure; (3) full phase changes (density and rheology). Such models were developed only recently (Burov et al., 2001; Gerya et al., 2002; Toussaint et al., 2004a,b; Burg and Gerya, 2005; Stöckhert and Gerya, 2005). In this particular study we search for upper bounds on the parameters controlling the continental subduction and thus UHP–HP exhumation. We consider the early stages of continental plate collision when subduction is assisted by high convergence rates and by the downward pull of the subducted oceanic slab.

2. Numerical model

We extended the Paro(a)voz code (Poliakov et al., 1993, Appendix) based on the FLAC (Fast Lagrangian Analysis of Continua) algorithm by Cundall (1989). This “2.5 D” explicit time-marching, large-strain Lagrangian algorithm locally solves Newtonian equations of motion in continuum mechanics approximation and updates them

in large-strain mode. The particular advantage of this code refers to the fact that it operates with full stress approximation, which allows for simple and accurate computation of total pressure, P , as a trace of the full stress tensor. The solution of these equations is coupled with constitutive and heat-transfer equations. Parovoz v9 also handles explicit elastic–ductile–plastic rheologies, free-surface boundary condition, full metamorphic changes, and surface processes (erosion and sedimentation (Avouac and Burov, 1996)). In Parovoz v9, the Lagrangian moving grid is backed by a much denser passive marker grid (in this study, 9 markers per grid element), which allows for diffusion-free interpolation of grid values, specifically stresses, between remeshings, as well as to track trajectories of selected particles to construct synthetic P – T – t paths.

3. Numerical problem setup

In the first series of experiments, we tested the classical case of stable oceanic subduction (Fig. 2a, top), where an oceanic plate subducts at a rate of 6 cm/yr below a continental plate (Yamato et al., 2007a). These experiments target the oceanic phase of the Alpine collision and are aimed, in particular, to test the idea of the possibility of tectonic overpressure in classical subduction settings, with account for density and rheological changes resulting from mineralogical phase transitions in the accretion prism and downgoing lithosphere. In these experiments, the thermo-mechanical model was fully coupled with a thermo-dynamic model using the reference thermodynamic algorithm THERIAK (De Capitani, 1994, see Appendix) that predicts mineralogical phases and their density by minimizing Gibbs energy for P – T conditions from the thermo-mechanical model (Parovoz). The changes in the physical properties are then re-iterated back to Parovoz.

3.1. Mechanical and thermal boundary conditions for oceanic subduction model

The choice of the mechanical boundary conditions follows the tradition of compatibility between the numerical and analog models. The upper boundary condition is a free surface. The lateral boundary conditions are kinematic (horizontal velocities). The Winkler's hydrostatic pliable bottom is used as the bottom boundary condition, in a slight difference from the rigid bottom condition used in analog models. This condition allows to reduce the vertical size of the model by up to 25% while keeping virtually the same behavior in the upper (lithospheric) domain. Semi-free Winkler's boundary

condition at the bottom and high competence contrast between the lithosphere and the underlying mantle ensure that the application of a constant horizontal velocity at the vertical borders does not prevent or assist a particular convergence mode: for the values of the sub-lithosphere mantle viscosity on the order of 5×10^{19} – 1×10^{20} Pa s, the deep mantle flow induced by the movement of the boundary produces negligible stresses at the base of the lithosphere. These stresses are below the threshold level of 0.1–0.01 MPa, which yields a mantle drag force per unit length of less than 10^{10} – 10^{11} N m⁻¹, i.e. 100 to 1000 times less than the slab push or pull force. In the subduction zones, the downward translation of a cold slab material produces complex thermal structures (Royden, 1993; Davies, 1999). To account for this complexity, in our model, the initial thermal structure relies on the oceanic plate cooling model for the oceanic part of the model (right side, Fig. 2a), while the continental part (left side) is based on the continental plate cooling model (Parsons and Sclater, 1977) with a thermotectonic age of 160 Ma. The corresponding thermal boundary conditions include zero flux in lateral direction, and fixed temperatures at the upper surface and the bottom of the model. For the entire model, the initial thermal distribution is computed from combination of the plate cooling models (oceanic or continental) for the upper lithospheric part with the adiabatic thermal gradient for the underlying mantle. We initially solve the plate cooling problem assuming $T=0$ °C at the surface and $T=1330$ °C at the bottom of the lithosphere. The initial adiabatic temperature gradient in the underlying mantle is computed by equalizing the temperature at its top with the temperature at the bottom of the lithosphere (1330 °C) and by adjustment the mantle heat flux in a way that the temperature at the bottom of the upper mantle (650 km depth) fits 2000 ± 100 °C (e.g., Turcotte and Schubert, 2002). We re-adjust the initial thermal thickness and, if necessary, the age of the plate to equalize heat fluxes at the mantle–lithosphere boundary. We control both the values of the surface and mantle heat flux to ensure that they fall in the expected range (30 – 80 mW m⁻² at the surface and 10 – 30 mW m⁻² in the mantle depending on plate age and thickness). The initial bottom and surface temperatures and zero lateral heat flow are kept fixed during the further computations. The particular difficulty of thermal computations in the accretion prism refers to the fact that the thermal conductivity in sedimentary materials varies from 1 to 5 W m⁻¹ K⁻¹, with low values for shales and sandstones ($\sim 1,2$ – $4,2$ W m⁻¹ K⁻¹) and higher values for limestones and dolomites (2 – 5 W m⁻¹ K⁻¹) (Turcotte and Schubert, 2002). The value used in standard (Std)

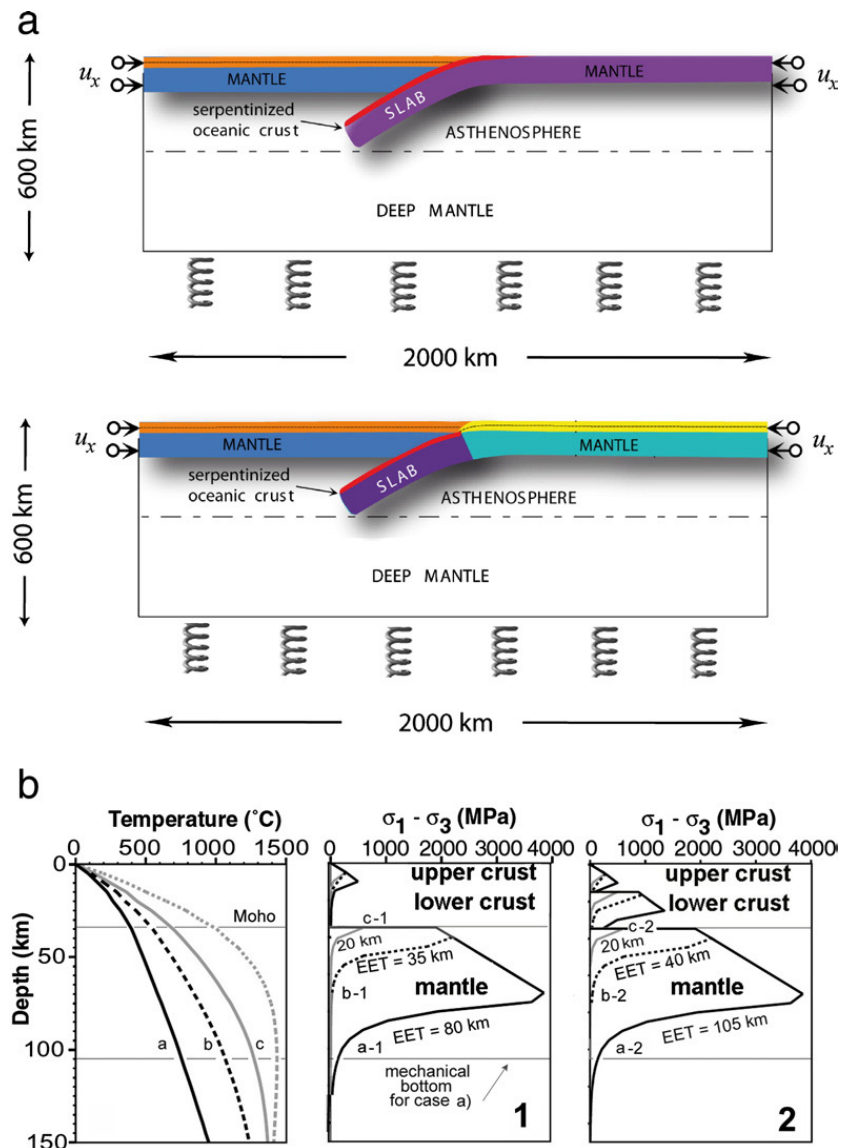


Fig. 2. a. Model setup. Numerical grid is composed of 1×1 km (oceanic experiments, top) or 5×5 km quadrilaterals (continental experiments, bottom). The upper boundary condition is a free surface combined with surface erosion and sedimentation in case of continental lithosphere. The bottom boundary condition is pliable Winkler basement. The lateral boundary conditions are velocities. The brittle–elastic–ductile rheology is different for the upper crust, lower crust, mantle lithosphere, slab, sediments, asthenosphere and deep mantle (Table 1, Fig. 2b). The model eclogites have the same rheology as the upper crust, but higher density (3400 kg/m^3). b. Representative thermal and rheology profiles for continental lithosphere as function of thermo-tectonic age. EET is Equivalent Elastic Thickness, proxy for the integrated strength of the lithosphere. Initial geotherms (left) and associated rheological strength profiles (middle and right) are computed for lithosphere with a 40-km-thick crust, deforming at a strain rate of 10^{-15} s^{-1} . Middle (1): Weak lower crust. Right (2): Strong lower crust. Black line: cold lithosphere (thermotectonic age=450 m.y., $T_{\text{Moho}}=400\text{--}450 \text{ }^\circ\text{C}$); black dashed lines: intermediate lithosphere (150 m.y., $550 \text{ }^\circ\text{C}$); gray line: hot lithosphere (75 m.y., $650\text{--}700 \text{ }^\circ\text{C}$); gray dashed line: very hot lithosphere (25 m.y., $1000 \text{ }^\circ\text{C}$).

simulation is $2 \text{ W m}^{-1} \text{ K}^{-1}$, but a twice higher thermal conductivity was also tested in the high thermal conductivity (Htc) experiment.

3.2. Mechanical and thermal boundary conditions for continental subduction model

In the second part of this study, we test continental collision assuming commonly referred initial scenario

(Fig. 2a, bottom). In this scenario, a rapidly subducting oceanic slab first entrains a very small part of a cold continental “slab”. In the model setup, there is no pre-imposed continental subduction. Instead, we pre-define a major thrust fault created by the preceding oceanic subduction and assume that the oceanic slab is still attached to the lower continental plate at the onset of the continental collision. The initial convergence rate equals the rate of the preceding oceanic subduction (two-sided initial

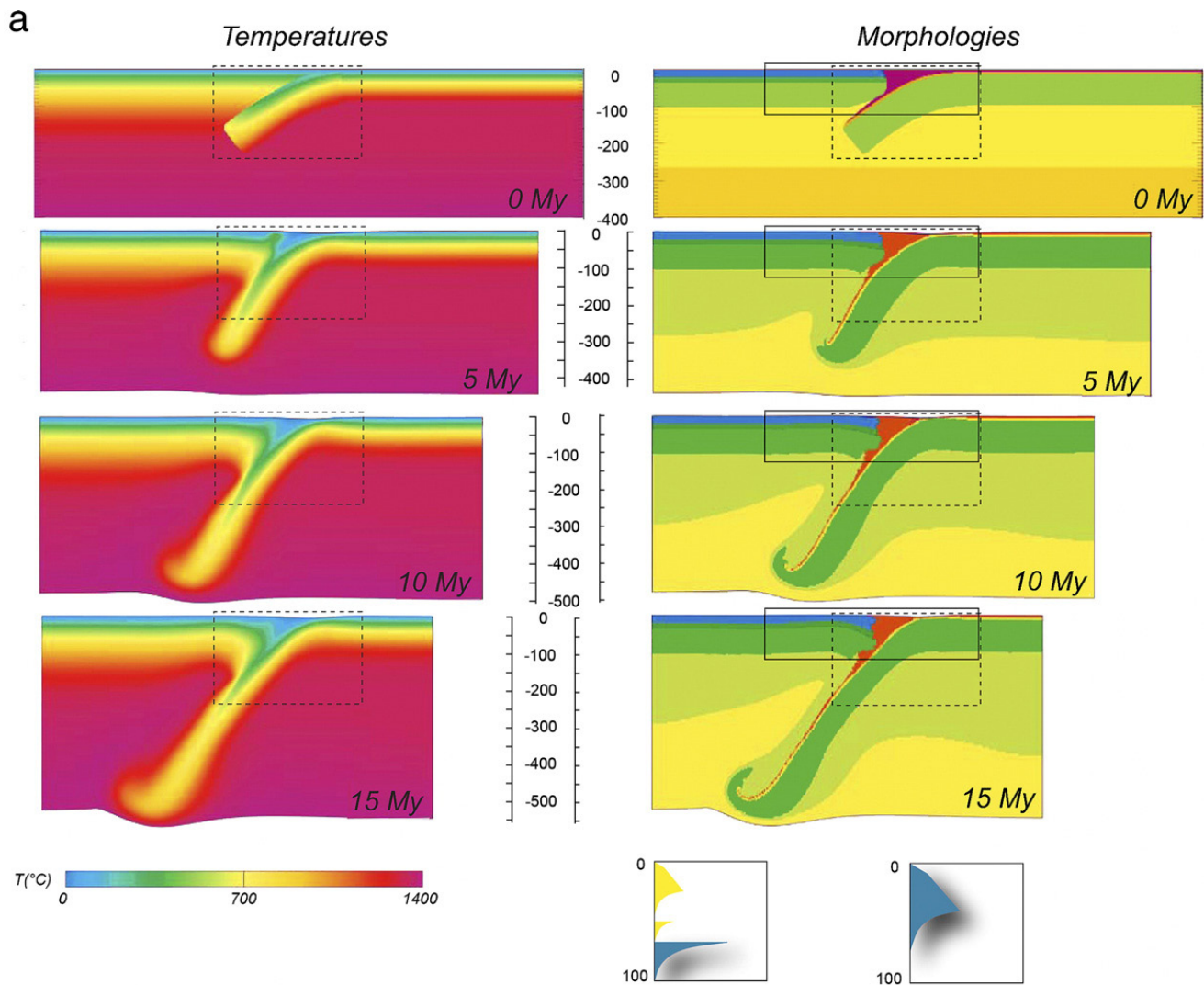


Fig. 3. a. Fully consistent oceanic subduction experiments equivalent to those published in (Yamato et al., 2007a), for the case of an oceanic plate subducting below a 160 Myr old continental lithosphere. This experiment referred below as “Std” implements thermo-dynamically consistent phase changes. Densities for all material phases are computed using the algorithm THERIAK (De Capitani, 1994; Table 1, Appendix). Squared zones show the position of zoom area shown in (b). Shown at the bottom are the assumed rheological profiles, for the continental (left) and oceanic plate (right). The profiles were derived for the mentioned thermotectonic age under assumption of quartz-rich upper continental crust, diabase lower crust, and olivine mantle (Table 1). Olivine is used for the entire oceanic lithosphere. b. Zoom to the subduction channel, for the experiments shown in (a). Marker field at 5 Myr (middle) traces the movements of the particles, which allows to trace P - T - t paths at each moment of time (bottom). In this model, exhumation of HP rocks was achieved at 10–13 Myr under assumption of low viscosity of the serpentinite layer. All markers used for the construction of the P - T - t paths were initially located in the normal (un-subducted) oceanic sediments (the uppermost 2 km layer of the crust). c. Pressure evolution in subduction channel for the experiments of Fig. 3 (Yamato et al., 2007a). Evolution of complete pressure as a function of depth is shown for experiments on oceanic subduction (Fig. 3). Within the accretion wedge i.e. above the bottom of the accretion wedge, there is no significant over- or under-pressure occurs, except for the experiment “Pel” (see below). At 80–100 km depth the presence of small over- and under-pressure can be attributed to variation in the thickness of the subduction channel and bending of the slab. Initial geotherms and associated rheological strength profiles for continental lithosphere (upper plate) are computed assuming a 35-km-thick crust. “Std” refers to pressure data for the reference experiment from (a). In order to test the influence of sediment density and bulk composition on the behavior of the accretion wedge, two different pelitic assemblages were considered (e.g., Spear, 1993). The first one is richer in Al and corresponds to a Garnet–Chlorite–Chloritoid simplified assemblage used in the Std simulation. “Pel” is a Garnet–Chlorite–Biotite simplified assemblage. This pelite density is computed in the “Pel” simulation and is slightly denser than the reference; the experiment “Ta_250” corresponds to one with 250 Ma old continental plate; “Htc” is the experiment with double thermal conductivity of sediment; experiment “Vis_m” explores a configuration with stronger lithosphere, in which A of the lithospheric mantle was reduced by a factor of 10. In order to test the influence of the sediment viscosity on the behavior of the accretion wedge, the pre-exponential material parameter A was multiplied by a factor of 10 in the experiment called “Vis_s”. In the experiment “Qtz”, lower crust was quartz dominated; in the experiments “Hvel” and “Lvel”, convergence rate for respectively twice and half of the convergence rate used in the reference experiment “Std”. d. Exhumation rates for the experiments shown in (c). The colors of the curves correspond to the colors used for different experiments described in caption to (c). Note two-stage character of exhumation. Initial exhumation rates are basically higher than on later stages.

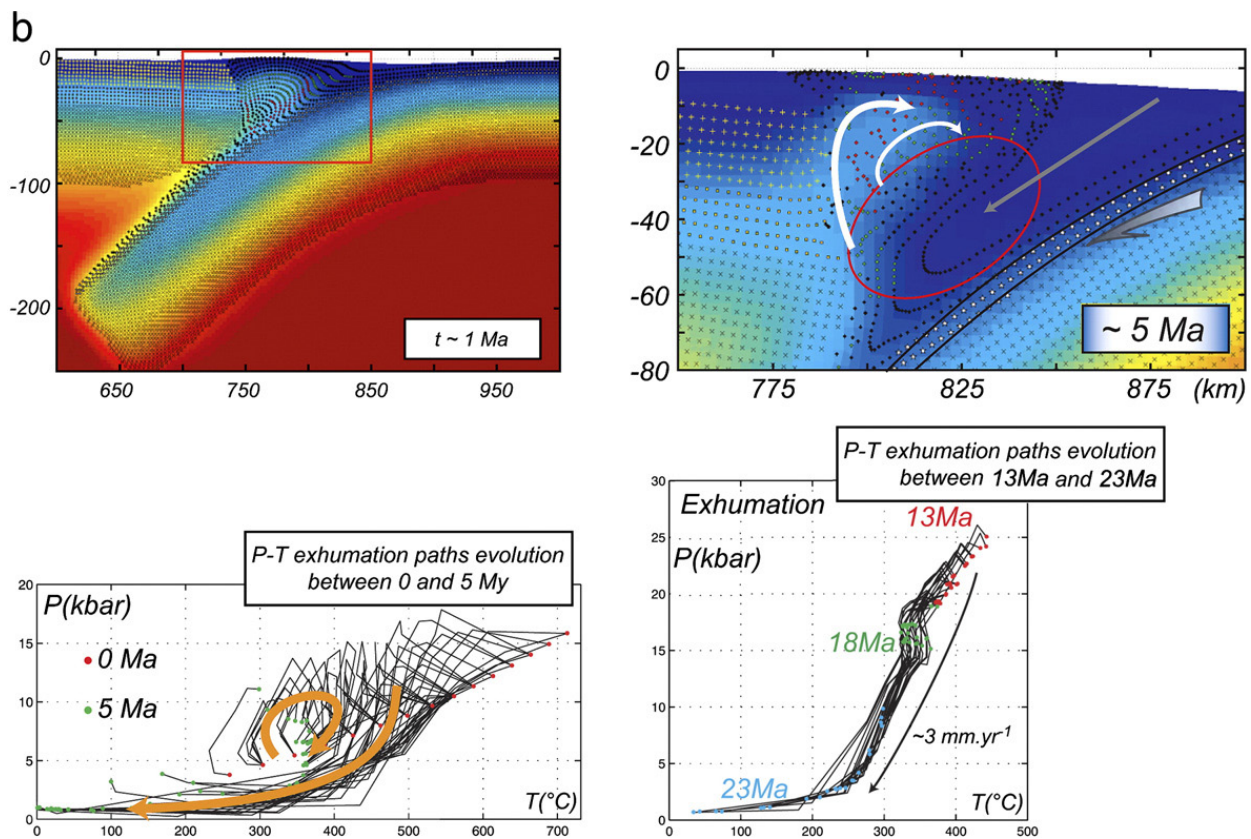


Fig. 3 (continued).

closing rate of 2×3 cm/yr during the first 5–10 m.y.). This rate (6 cm/yr) is on the order of the smallest present day oceanic subduction rates; it is also smaller than the average convergence rates deduced for some active continental collisions such as the India–Asia collision (2×4 to 2×5 cm/yr during the first 10 m.y. (Patriat and Achache, 1984). The initial thermal distribution is computed from the continental plate cooling model (Parsons and Sclater, 1977) assuming the same boundary conditions as for the oceanic experiments: fixed temperatures at surface and the bottom of the lithosphere (0°C and 1330°C , respectively) and zero outflow at the lateral sides. As before, we assume adiabatic temperature gradient for the upper mantle, which bottom is supposed to be at 2000°C .

3.3. Rheological structure

For continental and oceanic collision models, we use commonly inferred crustal structure and rheology parameters derived from rock mechanics (Table 1, Burov et al., 2001). As in nature, the topography growth is limited by surface erosion, which is modeled using diffusion erosion with diffusion coefficient of $500 \text{ m}^2 \text{ yr}^{-1}$ to

$1000 \text{ m}^2 \text{ yr}^{-1}$ (Burov et al., 2001). For continental collision, as for the case of the upper plate in the experiments on oceanic subduction, the initial geotherm is derived from the common half-space model (e.g., Parsons and Sclater, 1977).

3.4. Variable model parameters

The universal controlling variable parameter of all experiments is the initial geotherm, or thermotectonic age (Turcotte and Schubert, 2002), identified with the Moho temperature T_m (Fig. 2b). The geotherm or age defines major mechanical properties of the system, e.g., the rheological strength profile. By varying the geotherm, we account for the whole possible range of lithospheres, from very old, cold, and strong plates to very young, hot, and weak ones. The second variable parameter (for continental models) is the composition of the lower crust, which, together with the geotherm, controls the degree of crust–mantle coupling. We considered both weak (quartz dominated) and strong (diabase) lower-crustal rheology and also weak (wet olivine) mantle rheology (Table 1). Although we mainly applied a convergence rate of 2×3 cm/yr, we

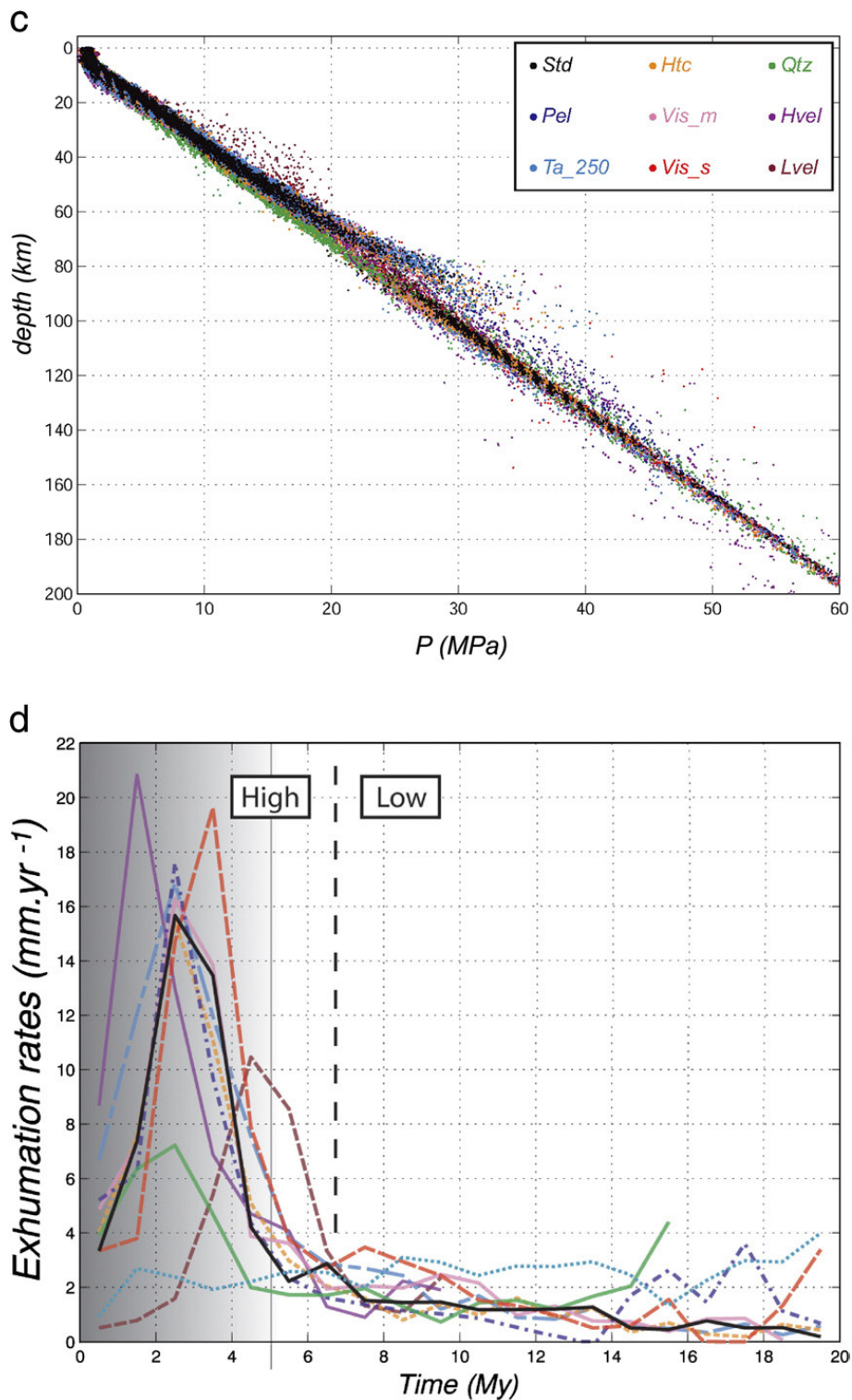


Fig. 3 (continued).

also tested smaller convergence rates (two times smaller, four times smaller, etc.). We tested the influence of most important metamorphic changes such as crustal eclogitization (at $P > 1.5$ GPa and $T > 550$ °C, see Table 1).

4. Oceanic subduction: fully thermo-mechanical and thermo-dynamically coupled experiments

As the mechanism of the oceanic subduction is not a subject of discussions itself, the main goal of the

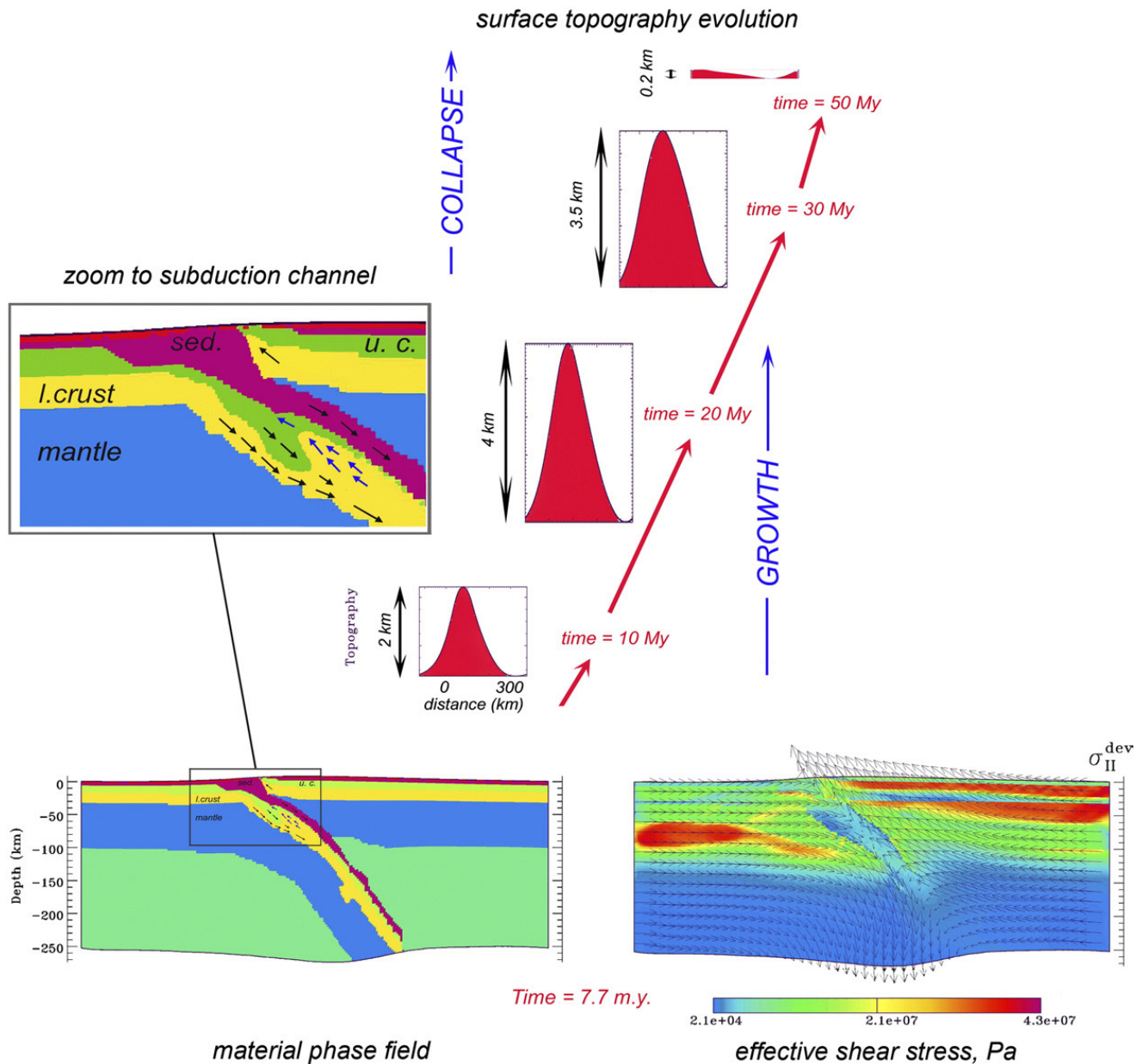


Fig. 4. Example of the model of continental collision and UHP exhumation in the Alpine collision context (Burov et al., 2001). The experiments refer to a slow convergence (6 mm/y) assuming that the continental lithosphere has been initially driven to the UHP depth (150 km) by the oceanic slab. With that assumption, the experiments show that once initialized, subduction may continue for 30–50 Myr. The convergence rate of 6 mm/y corresponds to the value that could be inferred for the Alps at the onset of collision, 5–10 Myr after the end of the preceding oceanic subduction. Surface topography is controlled by the erosion and sedimentation processes modeled using the linear diffusion erosion with a coefficient of diffusion of 500 m²/y (this value corresponds to stable mountain growth for given shortening rate, according to Avouac and Burov (1996)). The rest of the model design corresponds to the description provided in the section “Numerical model”, yet, with the important difference that in this particular case the continental subduction was prescribed from the beginning because the experiment was mainly focused on the mechanisms of exhumation of HP and UHP rocks and also tested the stability of the continental subduction process. The thermo-tectonic age of the lithosphere is 150–175 Myr, similar to the age used for the oceanic phase of subduction in the experiments shown in Fig. 3 (see the section “Numerical model” for more details). Shown are the material phase field, effective shear stress, velocity field, and topography evolution through time. The provided snapshot corresponds to 7.7 m.y. since the beginning of the experiment, when the exhumed UHP material started to arrive to the surface. Note that the images are cut from below following the grid elements that were initially at a 250 km depth.

“oceanic” experiments was to test P – T conditions in a fully-consistent model that accounts for all, realistic rheology, thermo-mechanical and thermodynamic cou-

pling. In the model (Fig. 3a), the oceanic crust is being transformed at corresponding P – T conditions ($P < 15$ kbar; $T < 500$ °C) to a weak serpentinite layer

(with effective viscosity cut off at 10^{18} Pa s), which results in a strength drop to fractions of MPa. We also assume that the fluid pressure is present in the serpentinite layer. This reduces its brittle strength by nearly a factor of 2. The ductile and brittle weakening in the serpentinite layer assures lubrication of the subduction channel. The thermodynamic part of the model continuously computes possible phase transforms as a function of P – T conditions. The corresponding density changes are re-iterated into the thermo-mechanical code. Unfortunately, the lack of data on the rheology of the metamorphic facies does not allow us to do the same for the associated rheological changes. Only few known rheology changes are implemented: the rheology of serpentinite and of eclogite. For other metamorphic facies, we supposed that their rheology is not different from the rheology of the initial rock.

The previous section describes the numerical setup of the experiments. The Fig. 3 shows the results of the reference experiment “Std” (see previous section). This experiment demonstrates stable character of subduction and of the geometry of the accretion wedge (Fig. 3b) as well as of the shape of the predicted P – T – t paths. It also confirms the previous ideas that the thickness of the accretion wedge cannot exceed certain critical depth (40–60 km). After growing to this critical size, the sedimentary wedge separates onto the “upper prism” (or wedge) and a deep crustal pocket (see snapshots at 10 and 15 Myr, Fig. 3a). This phenomenon was previously demonstrated by Burov et al. (2001) for the continental phase of Alpine collision. The deep crustal pocket presents a source for exhumation of HP and UHP rocks. It is noteworthy that the predicted pressure conditions in the subduction channel do not significantly deviate from the lithostatic gradient (Fig. 3c). Little under- and over-pressures occur in the subduction channel at depths >80 km. Some insignificant overpressures ($<20\%$) were also obtained at 40 km depth and refer to the bottom of the accretion wedge. It is also important that the exhumation rates are initially significantly higher than on later stages (Fig. 3d).

5. Continental collision. Experiments with a weak lower crust or mantle

Preliminary studies of continental collision in the Western Alps (Burov et al., 2001) have shown (Fig. 4) that continental subduction, once initialized, may continue for a quite a long period of time and result in multistage UHP exhumation described in the Introduction (see also Fig. 1b). These experiments, shown in Fig. 4, refer to

slow convergence rate (6 mm/y) assuming that the continental lithosphere has already subducted to the UHP depth before the onset of the experiments. Since the viability of this wishful assumption needs verification, in the following sections we present more advanced experiments where subduction of the continental lithosphere was not predefined (Fig. 2a). These numerical tests have also confirmed the idea (see Introduction) that a minimal initial convergence rate on the order of 3–5 cm/yr is needed for initialization of the continental subduction, and that it can be progressively reduced to 10 mm/yr within several My, with subduction still active.

5.1. Influence of the thermotectonic age or geotherm

In this set of experiments (Fig. 5 experiments “C”) we assumed common weak (quartz-dominated) lower-crustal rheology (“jelly-sandwich” rheology), relatively high initial convergence rate (2×3 cm/yr), and no phase changes. We also tested alternative “crème brûlée” rheology profiles (Burov and Watts, 2006) with strong lower crust (dry diabase) and weak wet olivine mantle rheology. Several types of collision scenarios were revealed as a function of thermotectonic age (geotherm) and rheology profile:

5.1.1. Cold geotherm ($T_m < 450$ °C, “jelly sandwich”)

An initially cold geotherm allows the collision to evolve into stable, oceanic-type subduction (Fig. 5, thermo-rheological profile “C₁”). Almost all shortening is accommodated by subduction both of the continental lower crust and mantle. Because of low Moho temperature, the lower crust is highly resistant to decoupling and keeps “welded” to the lithospheric mantle. It can be dragged to as deep as 250 km depth in spite of its positive buoyancy. However, the mechanical resistance of the major part of the upper crust remains lower than the buoyancy-induced stresses. It early separates from the lower crust and remains at surface or mid-crustal depth, only small amounts of the upper crust are dragged to the depth. In these experiments, crustal material is brought down to important depths (>120 – 150 km) allowing for UHP and HP metamorphism. This experiment closely resembles the experiment of Toussaint et al. (2004a) that modeled the India–Asia collision, but for rheology parameters adopted in Burov and Watts (2006). Fig. 6 shows formation of thrust-and-fold structures that are conditioned by the crust–mantle decoupling and resemble those typically observed in the field. This process explains eventual complexity of the recorded P – T – t paths. Fig. 7 shows non-lithostatic pressure field in the upper 250 km of the model. As can be seen, the subduction channel does not manifest any significant overpressure. Underpressure zones due to bending

of the lower plate are observed down to the depth of 100–150 km. Overpressure builds up in the mantle lithosphere only outside the subduction channel. This suggests that pressure recorded by the UHP–HP rocks exhumed in this context will correspond to the lithostatic pressure thus allowing to estimate their burial depth.

5.1.2. Intermediate geotherm ($T_m = 450\text{--}600\text{ }^\circ\text{C}$, “jelly sandwich”)

Stable subduction of the lithospheric mantle leads the lower crust to decouple from the mantle (Fig. 5, thermo-rheological profile “C”). For the intermediate geotherms, shortening is still largely accommodated by subduction, but the positively buoyant lower crust separates from the negatively buoyant lithospheric mantle and stagnates at some intermediate level (between 100 and 200 km), sometimes forming a double crustal zone (possible analogy is Northern Apennines, [Ponziani et al., 1995](#)). The crustal channel is divided onto the accretion prism and a lower crustal “pocket”. The geometry of the down-going lithospheric mantle is affected by the ascent of the buoyant lower crust: the slab adopts a very low angle of subduction. As a consequence, the oceanic slab detaches and sinks into the deep mantle. Small-amplitude (1000 m) long-wavelength (350–400 km) lithospheric folding also accommodates some part of the shortening, specifically in the upper plate. The crustal material is brought down to 100–120 km depth allowing for UHP and HP metamorphism.

5.1.3. Hot geotherm ($T_m = 600\text{--}700\text{ }^\circ\text{C}$, “jelly sandwich”)

Subduction and pure-shear thickening (Fig. 5, thermo-rheological profile “C₋₁”) are the results of collision under the conditions of a hot geotherm. At a Moho temperature of 650 °C, pure-shear thickening and moderate-amplitude (1500 m) lithospheric folding (wavelength 200–250 km) accommodate a significant part of shortening. This behavior is a result of the thermally induced weakening of the lithosphere that makes volumetric thickening mechanically easy. The base of the overriding lithospheric plate also weak as well and can be dragged downward with the sinking lower plate. The crustal

material basically does not arrive to depths larger than 60–80 km.

5.1.4. Very hot geotherm (“jelly sandwich”) or weak mantle (“crème brûlée”, $T_m > 750\text{ }^\circ\text{C}$ for weak lower crust and dry olivine mantle, or $T_m > 600\text{ }^\circ\text{C}$ for wet or dry diabase lower crust and wet olivine mantle)

Pure-shear thickening and RT instabilities (Fig. 5, thermo-rheological profiles “D” and “B” dubbed “crème brûlée” ([Burov and Watts, 2006](#)) result from very hot geotherms. For such a hot, weak lithosphere, stable subduction and lithospheric folding are impossible: convergence at the borders is entirely accommodated by pure-shear thickening and RT instabilities. Because of high temperatures, the effective viscosity at the base of the lithosphere is reduced, whereas its density is still higher than that of the asthenosphere; these two factors promote rapid (in <1 m.y.) development of RT instabilities. The slab thins in a “chewing gum” manner, and a “cold spot” forms (possible natural examples: Vrancea body in the Romanian Carpathians, e.g., [Wenzel, 2002](#); [Cloetingh et al., 2004](#)). The rate of “subduction” in this case is not controlled by the convergence rate but by the internal growth rate of the RT instability. We call this style of deformation “unstable subduction.”. In the conditions of these experiments, the crust is not brought down to any important depth (i.e. below 40 km).

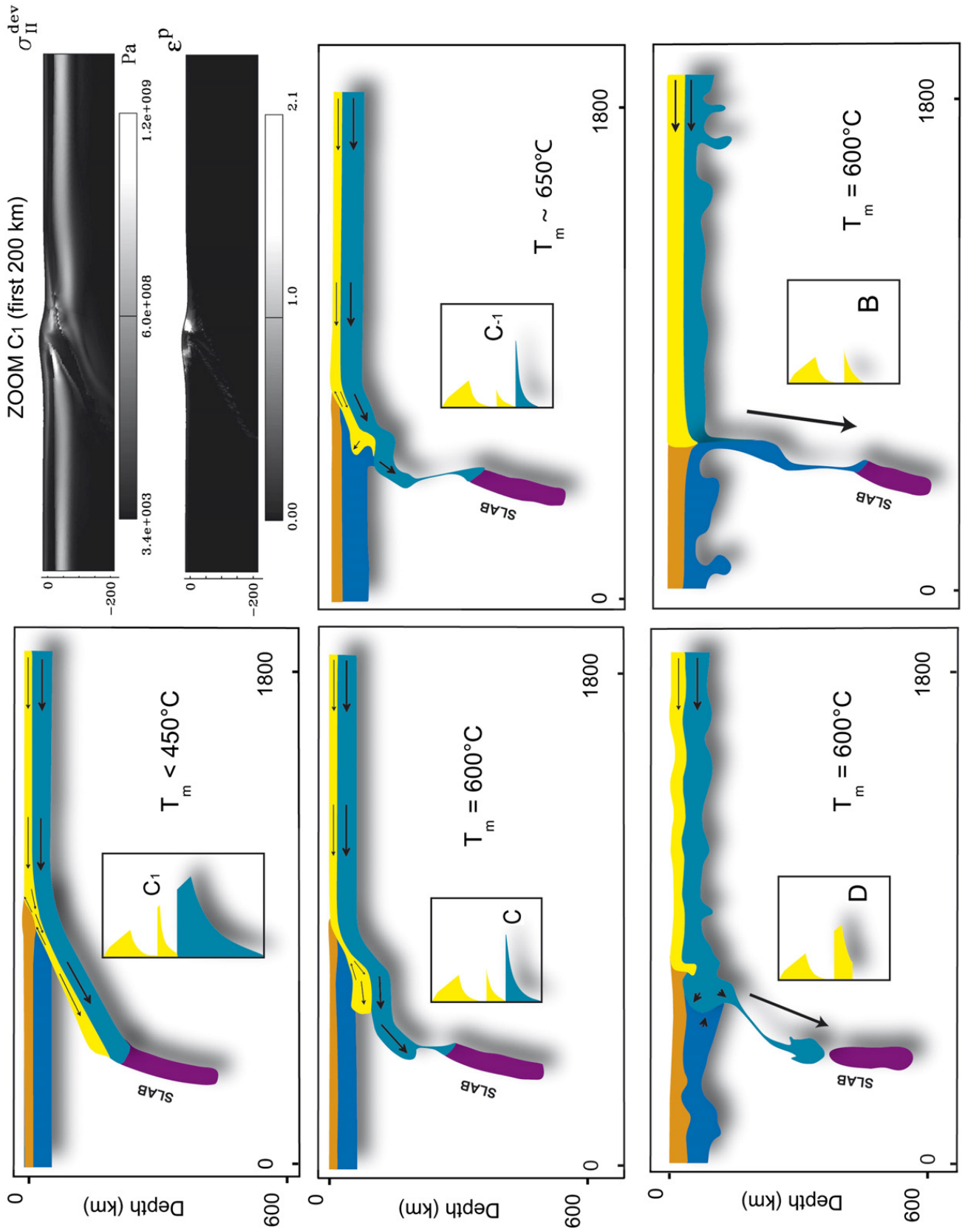
5.2. Influence of convergence rate

At smaller convergence rates (<5 cm/yr), continental subduction is still possible in “cold” cases ($T_{\text{Moho}} < 450\text{ }^\circ\text{C}$), whereas for intermediate-temperature and hot lithospheres, internal shortening dominates as a consequence of more effective conductive heating and, consequently, weakening of the lithosphere at decreasing convergence rates.

5.3. Influence of metamorphic changes

The major effect of UHP metamorphic changes (eclogitisation) appeared to be a steeper subduction

Fig. 5. Experiments on continental convergence assuming “jelly-sandwich” rheology with weak (quartz-rich) lower crust (experiments “C”), as well as the experiments based on the “crème brûlée” rheology with strong lower crust but weak lower mantle (“D” and “B”). Snapshots at 5.5 m.y., convergence rate 2×3 cm/yr, different rheology profiles. Moho temperatures are, respectively, 450 °C, 600 °C, 650 °C (profiles C₁, C, C₋₁), and 600 °C (profiles D and B). Profiles C correspond to dry olivine mantle, wet quartz-rich upper crust and wet diabase lower crust. Profile D corresponds to the hypothesis of ([Mackwell et al., 1998](#)) that combines common wet quartz rheology for the upper crust with uncommonly strong dry diabase rheology for the lower crust and a very weak olivine rheology for the mantle (wet olivine). The profile C₁ was used in [Toussaint et al. \(2004a\)](#) to model the initial stages of India–Asia collision. Profile B is similar to the profile D, but the lower crust is composed of wet diabase. The length of arrows is proportional to material velocity. The insert shows the effective shear stress and strain rate distribution for the central part of the “Indian” experiment C₁. These experiments resemble those from ([Toussaint et al., 2004a](#)) with a difference that this time we did not pre-define initial continental subduction and have updated the rheological profiles.



angle of the continental slab. The experiments suggest that phase changes do not significantly improve chances for “normal” subduction: when the Moho temperature exceeds 550–600 °C (temperature of onset of UHP metamorphism), subduction is not a dominant mechanism, whatever the degree of metamorphism is. Yet this is valid for the assumption of weak eclogite rheology (same as quartz rheology) used in the experiments. Any assumptions on eclogite rheology may be questioned because it is not well constrained. Additional experiments hint that the assumption that eclogite has a strong rheology (that of diabase) would be equivalent, in terms of mechanical behavior, to a shift of T_{Moho} by about –200 °C, which improves chances for continental subduction.

6. Continental collision. Experiments with strong lower crust and strong mantle

The experiments of the previous section were repeated assuming strong diabase rheology for the lower crust (Fig. 8). The resulting end-member scenarios (stable subduction vs. unstable subduction) are roughly the same as in the previous experiments. Yet, there are noticeable differences in the intermediate cases.

6.1. Cold lithosphere

For experiments with very cold lithospheres ($T_m < 450$ °C), the convergence yields stable subduction (Fig. 8). However, the results of this experiment differ in many ways from homologue experiments with weak lower crust. In this case, subduction involves the entire continental crust, including the upper crust and its sedimentary rocks. The lithosphere also has a much higher tendency for folding.

6.2. Intermediate-temperature lithospheres

For higher Moho temperatures ($T_m = 450$ – 750 °C), stable subduction is progressively replaced by pure-shear thickening and by large-scale lithospheric folding (Fig. 8). Folding is favored by the stronger rheology of the lower crust, which ensures its mechanical coupling with the lithospheric mantle. Note that for the same temperature range, but for a weak lower crust, subduction was a dominant mechanism of deformation.

6.3. Very hot lithosphere

The results of very “warm” experiments ($T_m > 750$ °C) are similar to those with the weak lower crust (Fig. 5,

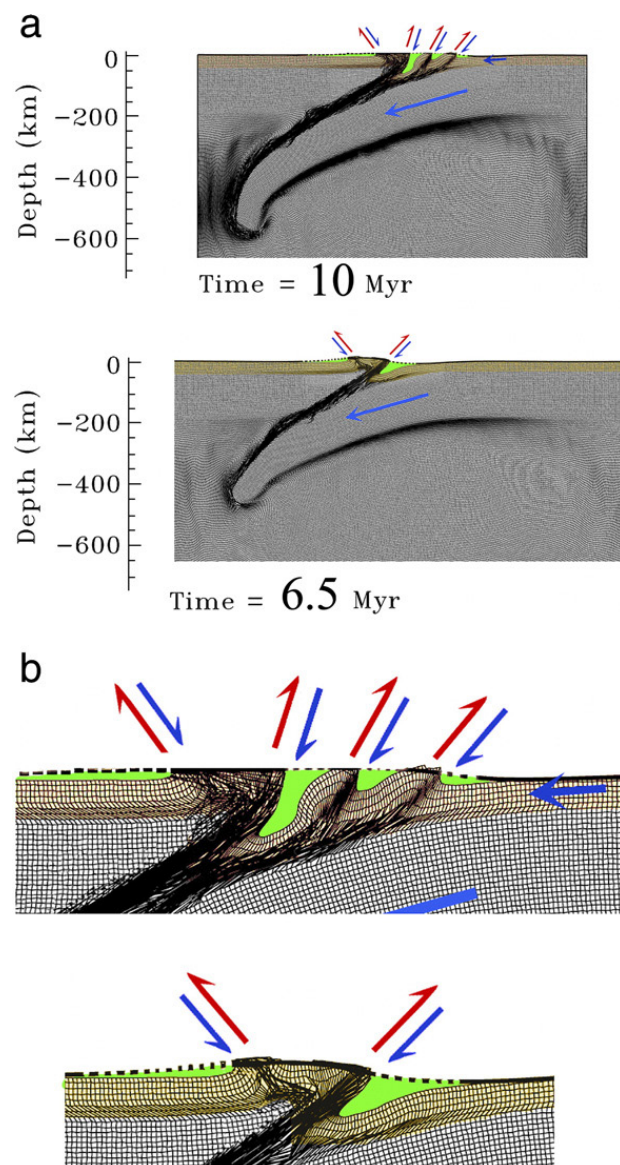


Fig. 6. a. Deformation of the marker grid highlighting multiple thrust-and-fold structures forming at different stages of continental subduction, for the experiment corresponding to the rheology profile “C₁” from Fig. 5. Formation of such structures requires a relatively low strength of the near-Moho zone in the lower crust (possibility of crust–mantle decoupling) and a strong mantle as sliding surface. This process explains eventual complexity of some of the resulting P – T – t paths. For the sake of space, the image is cut horizontally at 650 km depth (the bottom is not shown). Purple color corresponds to sedimentary deposits. b. Zoom to the central part of (a). Green color corresponds to the created sedimentary matter, orange color marks the upper crustal material, red color marks the lower crustal material. The gradation of the scale bar is 50 km.

profile B): unstable continental subduction and pure-shear thickening.

7. Discussion and conclusions

We considered here only simple collision scenarios. Account for pre-existing structures such as young

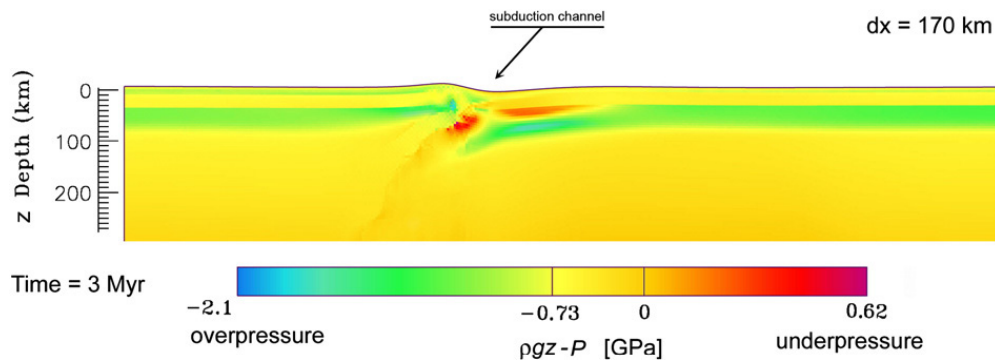


Fig. 7. Non-lithostatic pressure distribution within and around the subduction channel, for the experiment on “Indian-type” continental convergence (Fig. 5, profile C₁ or Toussaint et al., 2004a).

oceanic plates or ridges would require case-by-case justification of selected model geometries.

The collision mode is conditioned by the initial convergence rate and the thermo-rheological state of the lithosphere. The results (summarized in Figs. 5 and 9) suggest a wide variety of scenarios for development of young collision zones and their poly-phase character. The continental subduction (1) and thus HP–UHP exhumation is possible only in case of strong mantle lithospheres characterized by Moho temperatures below $T_m < 550^\circ\text{C}$ and relatively fast initial convergence rates ($> 5\text{ cm/yr} < 15\text{ cm/y}$). Since the critical values of the convergence rates are close to normal oceanic subduction rates, it is reasonable to assume that most continental collision zones might have went through a continental subduction phase at the initial stages (5–10 Myr) of their evolution. In the

case of weaker mantle lithospheres (or slower convergence rates), alternative deformation mechanisms prevail: (2) lithospheric folding ($500^\circ\text{C} < T_m < 650^\circ\text{C}$); (3) pure-shear thickening ($550^\circ\text{C} < T_m < 650^\circ\text{C}$), and (4) RT instabilities ($T_m > 650^\circ\text{C}$). In some cases, folding may also develop in case of overall strong rheology and fast convergence rate.

Strong diabase lower crust may allow for entrainment of light upper crust and sediments to a great depth (200 km), which is the domain of HP–HT (high pressure–high temperature) and UHP–UHT (ultrahigh pressure–ultrahigh temperature) metamorphism. The metamorphism influences deep slab geometry, but does not promote stable subduction in the case of weak eclogite rheologies. Yet, it probably does so in the case of strong eclogite rheologies.

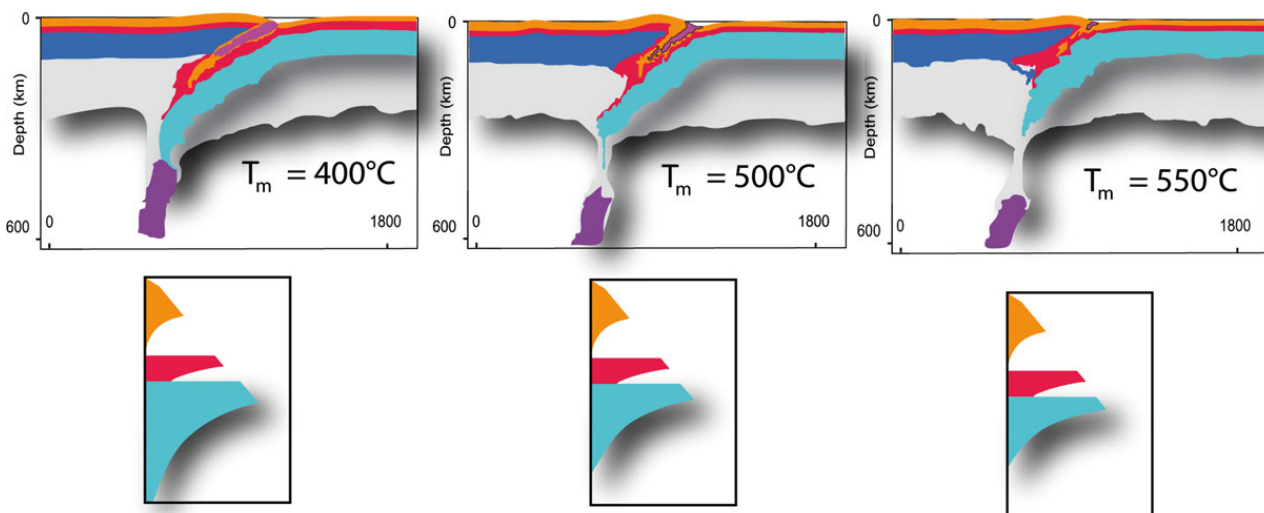


Fig. 8. Experiments with strong dry diabase lower crust (quartz–diabase–dry olivine rheology) at 5.5 m.y. Moho temperatures are respectively 400°C , 500°C and 550°C . All other parameters and details are as in the experiments from the Fig. 5. Note important buckling of the plates imposed by the presence of strong diabase crust that results in mechanical coupling between the plates. Purple color corresponds to the sedimentary matter or to the oceanic slab, orange color marks the upper crustal material, red color marks lower crustal material. Blue (dark or light) color marks mantle lithosphere; grey color marks asthenosphere.

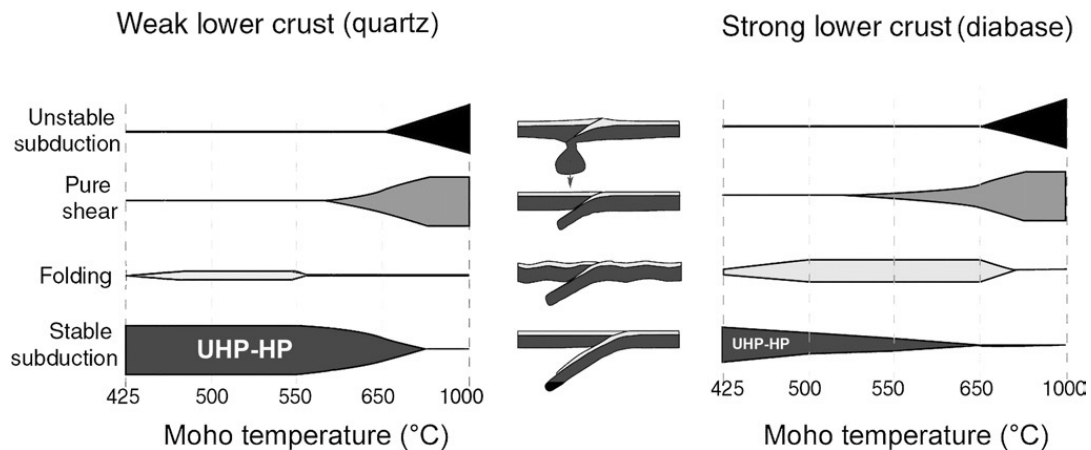


Fig. 9. Summary of observed continental convergence scenarios. Diagrams show contribution of each particular deformation mechanism. Lithostatic UHP exhumation is mainly associated with subduction whereas possible overpressure is associated with folding mode.

The experiments show that the assumption of a weak mantle rheology is incompatible with formation and exhumation of HP and UHP material, because a strong mantle is minimum needed to force the positively buoyant crust to depth. For the alternative rheology profiles comprising, for example, a strong crust but a weak mantle (“crème brûlée”), the compression results in large-scale crustal folding, not in subduction or collision. Such system becomes rapidly destabilized due to advection of hot asthenospheric material directly to the base of the crust. It thus appears that in most cases of continental convergence, both the upper and the lower plates should have a variant of the “jelly sandwich” rheology characterized by a strong mantle that serves as (1) a guide for tectonic stress, (2) a strong base needed to drive the crustal material down and up, and (3) a shield protecting the base of the crust from direct contact with the hot asthenosphere.

The exhumation of UHP rocks thus may be produced by different mechanisms: (1) the LP and MP rocks can be exhumed via the “normal” accretion prism mechanism. (2) the HP and UHP rocks can be exhumed, as suggested in Burov et al., 2001, as a result of small scale convection in the deep crustal “pocket” created by separation of the subducting crust from the mantle below 80–120 km depth. The metamorphic rocks are brought up by this mechanism to 40–50 km depth, to the base of the deep accretion prism. From there they may be further ascent by the accretion prism mechanism. Small scale convection in the deep crustal pocket and subduction channel is conditioned by viscosity drop and floatability rise due to (1) heat transfer from the asthenosphere below the upper plate; (2) shear heating; (3) viscosity drop due to metamorphic reactions; (4) additional heating due to radioactive heat sources carried down with the sediments and

the upper crustal material, (5) dehydration and other case-specific mechanisms (Gerya et al., 2008). The efficiency of the proposed mechanism depends on the degree of metamorphism, i.e. on the mean density of the metamorphic rocks.

As suggested by Stöckhert and Gerya (2005), it is also not excluded that convective crustal instability is complemented by diapiric (RT) instability that can brought a part of the material vertically, avoiding the subduction channel, which may result in exhumation in the backstop area (for low–middle pressure facies backstop exhumation may be purely kinematic).

In specific cases (small volumes of undeformed UHP rock), the rigid crustal block exhumation model (Chemenda et al., 1995) may be also applicable. However, this model needs a thermo-mechanical validation.

Subduction channel is devoid of significant deviations from lithostatic pressure gradient. Small underpressures may be produced at depths below 40–50 km. The surrounding lithosphere may be both under- and over-pressured with pressures reaching up 1.6–2 times lithostatic. Nevertheless, the zones of anomalous pressure do not participate in the exhumation turnover. Consequently, in most cases, UHP P – T – t data can be decoded in terms of the exhumation depth using lithostatic pressure assumptions.

Acknowledgements

We thank Parovoz co-builders, Y. Podladchikov, for the critical impulse, and A. Poliakov, for the absence of such, and T. Gerya for pushing us hard to advance with this study. The reviewers, S. Cloetingh and S. Buiter are deeply thanked for in-depth reviews and many critical constructive comments and corrections.

Appendix A. Numerical algorithm

Thermo-mechanical-module

This mixed finite-element volume/finite difference code Parovoz is based on the FLAC technique (Cundall, 1989). It solves simultaneously Newtonian dynamic equations of motion (A1), in a Lagrangian formulation, coupled with visco-elasto-plastic constitutive Eq. (A2), heat transport Eq. (A3) and state Eq. (A4) (see Appendix A, (e.g., Burov and Guillou-Frotier, 1999; Burov et al., 2001; Le Pourhiet et al., 2004) for details concerning numerical implementation).

$$\left\langle \rho \frac{\partial^2 \mathbf{d}}{\partial t^2} \right\rangle - \text{div} \sigma - \rho \mathbf{g} = 0 \quad (\text{A1})$$

$$\frac{D\sigma}{Dt} = F(\sigma, \mathbf{u}, V, \nabla V, \dots T \dots) \quad (\text{A2})$$

$$\rho C_p \partial T / \partial t + \mathbf{u} \nabla T - k \text{div}(\nabla T) - H_r - \text{frac} \times \sigma_{\text{II}} \partial \varepsilon_{\text{II}} / \partial t = 0 \quad (\text{A3})$$

assuming adiabatic temperature dependency for density and Boussinesq approximation for thermal body forces:

$$\rho = \rho_0(1 - \alpha \Delta T) \quad (\text{A4})$$

Here \mathbf{d} , \mathbf{u} , σ , \mathbf{g} , k are the respective terms for displacement, velocity, stress, acceleration due to body forces and thermal conductivity. The brackets in Eq. (A1) specify conditional use of the related term: in quasi-static mode, the inertia is dumped using inertial mass scaling (Cundall, 1989). The terms t , ρ , C_p , T , H_r , α , $\text{frac} \times \sigma_{\text{II}} \partial \varepsilon_{\text{II}} / \partial t$ designate respectively time, density, specific heat, temperature, internal heat production, thermal expansion coefficient and shear heating term moderated by experimentally defined frac multiplier (frac was set to 0 in our experiments). The terms $\partial / \partial t$, $D\sigma / Dt$, F are a time derivative, an objective (Jaumann) stress time derivative and a functional, respectively. In the Lagrangian framework, the incremental displacements are added to the grid coordinates allowing the mesh to move and deform with

the material. This enables solution of large-strain problems locally using small-strain formulation: on each time step the solution is obtained in local coordinates, which are then updated in the large strain mode. Volume/density changes due to phase transitions are accounted via application of equivalent stresses to affected material elements.

Solution of Eq. (A1) provides velocities at mesh points used for computation of element strains and of heat advection $\mathbf{u} \nabla T$. These strains are used in Eq. (A2) to calculate element stresses, and the equivalent forces are used to compute velocities for the next time step.

All rheological terms are implemented explicitly. The rheology model is serial viscous–elastic–plastic (Table 1). The plastic term is given by explicit Mohr–Coulomb plasticity (non-associative with zero dilatancy) assuming linear Navier–Coulomb criterion. We imply internal friction angle ϕ of 30° and maximal cohesion S of 20 Mpa, which fit best the experimental Byerlee’s law of rock failure (Byerlee, 1978):

$$\tau = S + \sigma_n \tan \phi \quad (\text{A5})$$

where τ is the shear stress and σ_n is the normal stress. Linear cohesion softening is used for better localization of plastic deformation ε_p ($S(\varepsilon_p) = S_0 \min(0, 1 - \varepsilon_p / \varepsilon_{p0})$ where ε_{p0} is 0.01). Specific properties are applied to soft serpentinised rock (Hassani et al., 1997).

The ductile–viscous term is represented by non-linear power law with three sets of material parameters (Table 1) that correspond to the properties of four lithological layers: upper crust (quartz), middle–lower crust (quartz–diorite), mantle and asthenosphere (olivine):

$$\eta_{\text{eff}} = \left(\frac{\partial \varepsilon}{\partial t} \right)_{\text{II}}^{d(1-n)/n} (A^*)^{-1/n} \exp(H/nRT) \quad (\text{A6})$$

where $\left(\frac{\partial \varepsilon}{\partial t} \right)_{\text{II}}^d = \left(\text{Inv}_{\text{II}} \left(\left(\frac{\partial \varepsilon}{\partial t} \right)_{\text{II}}^d \right) \right)^{1/2}$ is the effective strain rate and $A^* = 1/2 A \cdot 3^{(n+1)/2}$ is the material constant, H is the activation enthalpy, $H = Q + PV$ where Q is activation energy and V is molar volume, R is the gas constant, n is the power law exponent (Table 2). The elastic parameters

Table 2
Summary of ductile flow parameters assumed in model calculations^a

	Composition	Pre-exponential stress constant A MPa ⁻ⁿ s ⁻¹	Power law exponent n	Activation energy, Q KJ mol ⁻¹
Upper Crust	Wet Quartzite	1.1 × 10 ⁻⁴	4	223
Lower Crust	Dry Maryland Diabase	8 ± 4	4.7 ± 0.6	485 ± 30
	Undried Pikwitonei granulite	1.4 × 10 ⁴	4.2	445
Mantle or Oceanic lithosphere	Dry Olivine	4.85 × 10 ⁴	3.5	535
	Wet Olivine	417	4.48	498

^a The failure envelopes in this paper match those in Mackwell et al. (1998) derived from Gleason and Tullis (1995), Wilks and Carter (1990), Hirth and Kohlstedt (1996), Chopra and Paterson (1981).

(Table 1) correspond to commonly inferred values from Turcotte and Schubert (2002).

In addition, surface processes are taken into account by diffusing Eq. (A7) the topographic elevation h of the free surface along x using conventional Culling erosion model (Culling, 1960) with a diffusion coefficient k_{ero} .

$$\frac{\partial^2 h}{\partial t^2} = k_{\text{ero}} \frac{\partial^2 h}{\partial x^2} \quad (\text{A7})$$

This simple model is well suited to simulate fan deltas, which can be taken as a reasonably good analogue of typical foreland basin deposits. This model is not well adapted to model slope dependent long-range sedimentation, yet, it accounts for some most important properties of surface processes such as dependency of the erosion/sedimentation rate on the roughness of the relief (surface curvature).

PARA(O)VOZ allows for large displacements and strains in particular owing to an automatic remeshing procedure, which is implemented each time the mesh becomes too distorted to produce accurate results. The remeshing criterion is imposed by a critical angle of grid elements. This angle is set to 10° to reduce frequency of remeshing and thus limit the associated numerical diffusion. The numerical diffusion was effectively constrained by implementation of the passive marker algorithm. This algorithm traces passively moving particles that are evenly distributed in the initial grid. This allows for accurate recovering of stress, phase and other parameter fields after each remeshing. PARA(O)VOZ has been already tested on a number of geodynamical problems for subduction/collision context (Burov et al., 2001; Toussaint et al., 2004a,b).

Thermodynamic module

Buoyancy (and, eventually, rheology changes) is an important component of the force balance at subduction zone (Bousquet et al., 1997; Burov et al., 2001; Doin and Henry, 2001). For this reason, the thermodynamic THERIAK algorithm (De Capitani, 1994) has been incorporated to introduce progressive density changes during evolution. THERIAK minimizes free Gibbs energy for a given chemical composition to calculate an equilibrium mineralogical assemblage for given P – T conditions (De Capitani and Brown, 1987).

$$G = \sum_{i=1}^n \mu_i N_i \quad (\text{A8})$$

where μ_i is the chemical potential and N_i the moles number for each component i constitutive of the assemblage. Given the mineralogical composition, the computation of the density is then straightforward.

Mineralogical composition and hence density, is re-evaluated every 10^4 time steps (~ 200 kyr) according to the current P – T conditions. Equivalent stresses are applied to the elements to account for volume–density changes associated with the metamorphic transitions.

Unfortunately, changes in rheological properties of the metamorphic facies cannot be implemented in the same way as the density changes, due to the lack of the appropriate experimental data. We took into account rheology changes only for key facies such as serpentinite and eclogite.

References

- Agard, P., Jolivet, L., Goffé, B., 2001. Tectonometamorphic evolution of the Schistes Lustrés complex: implications for the exhumation of HP and UHP rocks in the Western Alps. *Bulletin de la Societe Geologique de France* 172 (5), 617–636.
- Artyushkov, E.V., 1973. Stresses in the lithosphere caused by crustal thickness inhomogeneities. *Journal of Geophysical Research* 78, 7675–7708.
- Austrheim, H., 1991. Eclogite formation and the dynamics of crustal roots under continental collision zones. *Terra Nova* 3, 492–499.
- Avouac, J.P., Burov, E.B., 1996. Erosion as a driving mechanism of intracontinental mountain growth. *Journal of Geophysical Research-Solid Earth* 101 (B8), 17747–17769.
- Beaumont, C., Kamp, P.J.J., Hamilton, J., Fullsack, P., 1996. The continental collision zone, South Island, New Zealand: comparison of geodynamical models and observations. *Journal of Geophysical Research* 101, 3333–3359.
- Beaumont, C., Muñoz, J.A., Hamilton, J., Fullsack, P., 2000. Factors controlling the Alpine evolution of the central Pyrenees inferred from a comparison of observations and geodynamical models. *Journal of Geophysical Research* 105 (B4). doi:10.1029/1999JB900390, 8121–8146.
- Bousquet, R., Goffé, B., Henry, P., Le Pichon, X., Chopin, C., 1997. Kinematic, thermal and petrological model of the Central Alps; Lepontine metamorphism in the upper crust and eclogitisation of the lower crust. *Tectonophysics* 273 (1–2), 105–127.
- Burg, J.-P., Gerya, T.V., 2005. Viscous heating and thermal doming in orogenic metamorphism: numerical modeling and geological implications. *Journal of Metamorphic Geology* 23, 75–95.
- Burg, J.-P., Podladchikov, Y., 2000. From buckling to asymmetric folding of the continental lithosphere: numerical modelling and application to the Himalayan syntaxes. In: Khan, M.A., et al. (Eds.), *Tectonics of the Nanga Parbat syntaxis and the western Himalaya*. Geological Society of London, Special Publication, 170, pp. 219–236.
- Burov, E.B., Diament, M., 1995. The effective elastic thickness (T_e) of continental lithosphere: what does it really mean? *Journal of Geophysical Research* 100, 3895–3904.
- Burov, E.B., Guillou-Frottier, L., 1999. Thermo-mechanical behaviour of large ash-flow calderas. *Journal of Geophysical Research* 104, 23081–23109.
- Burov, E.B., Molnar, P., 1998. Gravity anomalies over the Ferghana Valley (central Asia) and intracontinental deformation. *Journal of Geophysical Research* 103 (B8), 18137–18152.
- Burov, E., Watts, A.B., 2006. The long-term strength of continental lithosphere: “jelly-sandwich” or “crème-brûlée”? *GSA Today* 16, 4–10.

- Burov, E.B., Kogan, M.G., Lyon-Caen, H., Molnar, P., 1990. Gravity anomalies, the deep structure, and dynamic processes beneath the Tien Shan. *Earth and Planetary Science Letters* 96, 367–383.
- Burov, E., Jolivet, L., Le Pourhiet, L., Poliakov, A., 2001. A thermo-mechanical model of exhumation of high pressure (HP) and ultrahigh pressure (UHP) metamorphic rocks in Alpine-type collision belts. *Tectonophysics* 342, 113–136.
- Byerlee, J.D., 1978. Friction of rocks. *Pure and Applied Geophysics* 116, 615–629.
- Chemenda, A.L., Mattauer, M., Malavieille, J., Bokun, A.N., 1995. A mechanism for syn-collisional deep rock exhumation and associated normal faulting: results from physical modeling. *Earth and Planetary Science Letters* 132, 225–232.
- Chopin, C., 1984. Coesite and pure pyrope in high-grade blueschists of the western Alps: a first record and some consequences. *Contributions to Mineralogy and Petrology* 96, 253–274.
- Chopra, P.N., Paterson, M.S., 1981. The experimental deformation of dunite. *Tectonophysics* 78, 453–473.
- Cloetingh, S., Burov, E., 1996. Thermomechanical structure of European continental lithosphere: constraints from rheological profiles and EET estimates. *Geophysical Journal International* 124, 695–723.
- Cloetingh, S.A.P.L., Wortel, M.J.R., Vlaar, N.J., 1982. Evolution of passive continental margins and initiation of subduction zones. *Nature* 297, 139–142.
- Cloetingh, S., Burov, E., Poliakov, A., 1999. Lithosphere folding: primary response to compression? (from central Asia to Paris Basin). *Tectonics* 18, 1064–1083.
- Cloetingh, S.A.P.L., Burov, E., Matenco, L., Toussaint, G., Bertotti, G., Andriessen, P.A.M., Wortel, W.J.R., Spakman, W., 2004. Thermomechanical controls on the model of continental collision in the SE Carpathians (Romania). *Earth and Planetary Science Letters* 218, 57–76.
- Cloos, M., 1993. Lithospheric buoyancy and collisional orogenesis: subduction of oceanic plateaus, continental margins, island arcs, spreading ridges and seamounts. *Geological Society of America Bulletin* 105, 715–737.
- Culling, W.E.H., 1960. Analytical theory of erosion. *Journal of Geology* 68, 333–336.
- Cundall, P.A., 1989. Numerical experiments on localization in frictional material. *Ingenieur-Archiv* 59, 148–159.
- Dahlen, F.A., 1981. Isostasy and the ambient state of stress in the oceanic lithosphere. *Journal of Geophysical Research* 86, 7801–7807.
- Dahlen, F.A., 1990. Critical taper model of fold-and-thrust belts and accretionary wedges. *Annual Review of Earth and Planetary Science* 18, 55–99.
- Dahlen, F.A., Suppe, J., 1988. Mechanics, growth and erosion of mountain belts. *Special Paper — Geological Society of America* 218, 161–178.
- Davies, J.H., 1999. Simple analytic model for subduction zone thermal structure. *Geophysical Journal International* 139, 823–828.
- Davis, D.M., Suppe, J., Dahlen, F.A., 1983. Mechanics of fold-and-thrust belts and accretionary wedges. *Journal of Geophysical Research* 88 (B2), 1153–1172.
- De Capitani, C., Brown, T.H., 1987. The computation of chemical equilibrium in complex systems containing non-ideal solutions. *Geochimica et Cosmochimica Acta* 51, 2639–2652.
- De Capitani, C., 1994. Gleichgewichts-phasendiagramme: theorie und software. *Beihefte zum European Journal of Mineralogy-Jahrestagung der Deutschen Mineralogischen Gesellschaft* 48.
- Doin, M.-P., Henry, P., 2001. Subduction initiation and continental crust recycling: the roles of rheology and eclogitization. *Tectonophysics* 342, 163–191.
- Emerman, S.H., Turcotte, D.L., 1983. A fluid model for the shape of accretionary wedges. *Earth and Planetary Science Letters* 63, 379–384.
- England, P.C., Houseman, G.A., 1989. Extension during continental convergence, with application to the Tibetan Plateau. *Journal of Geophysical Research* 94, 17561–17579.
- Fleitout, L., Froidevaux, C., 1982. Tectonics and topography for a lithosphere containing density heterogeneities. *Tectonics* 1, 21–56.
- Fleitout, L., Froidevaux, C., 1983. Tectonic stresses in the lithosphere. *Tectonics* 3, 315–324.
- Gerya, T.V., Stoeckert, B., 2005. 2-D numerical modeling of tectonic and metamorphic histories at active continental margins. *International Journal of Earth Science*. doi:10.1007/s00531-005-0035-9.
- Gerya, T.V., Yuen, D.A., 2003. Rayleigh–Taylor instabilities from hydration and melting propel “cold plumes” at subduction zones. *Earth and Planetary Science Letters* 212, 47–62.
- Gerya, T.V., Stöckert, B., Perchuk, A.L., 2002. Exhumation of high-pressure metamorphic rocks in a subduction channel: a numerical simulation. *Tectonics* 26 (6), 1–15.
- Gerya, T.V., Perchuk, L.L., Burg, J.-P., 2008. Transient hot channels: perpetrating and regurgitating ultrahigh-pressure, high temperature crust–mantle associations in collision belts. *Lithos* 103, 236–256.
- Gleason, G.C., Tullis, J., 1995. A flow law for dislocation creep of quartz aggregates determined with the molten salt cell. *Tectonophysics* 247, 1–23.
- Goetze, C., Evans, B., 1979. Stress and temperature in the bending lithosphere as constrained by experimental rock mechanics. *Geophysical Journal of the Royal Astronomical Society* 59, 463–478.
- Gorczyk, W., Gerya, T.V., Connolly, J.A.D., Yuen, D.A., Rudolph, M., 2006. Large-scale rigid-body rotation in the mantle wedge and its implications for seismic tomography. *Geochemistry Geophysics Geosystems* 7 (Q05018). doi:10.1029/2005GC001075.
- Hassani, R., Jongmans, D., Chery, J., 1997. Study of plate deformation and stress in subduction processes using two-dimensional numerical models. *Journal of Geophysical Research* 102 (B8), 17951–17965.
- Hirth, G., Kohlstedt, D.L., 1996. Water in the oceanic upper mantle: implications for rheology, melt extraction and the evolution of the lithosphere. *Earth and Planetary Science Letters* 144, 93–108.
- Houseman, C.A., Molnar, P., 1997. Gravitational (Rayleigh–Taylor) instability of a layer with nonlinear viscosity and convergence thinning of continental lithosphere. *Geophysical Journal International* 128, 125–150.
- Jolivet, L., Daniel, J.M., Truffert, C., Goffé, B., 1994. Exhumation of deep crustal metamorphic rocks and crustal extension in back-arc regions. *Lithos* 33, 3–30.
- Kirby, S.H., Durham, W., Stern, L., 1991. Mantle phase changes and deep-earthquake faulting in subducting lithosphere. *Science* 252, 216–225.
- Lavier, L., Steckler, M., 1997. The effect of sedimentary cover on the flexural strength of continental lithosphere. *Nature* 389, 476–479.
- Le Pichon, X., Fournier, M., Jolivet, L., 1992. Kinematics, topography, shortening and extrusion in the India–Eurasia collision. *Tectonics* 11, 1085–1098.
- Le Pourhiet, L., Burov, E., Moretti, I., 2004. Rifting through a stack of inhomogeneous thrusts (the dipping pie concept). *Tectonics* 23 (4). doi:10.1029/2003TC001584. TC4005.
- Mackwell, S.J., Zimmerman, M.E., Kohlstedt, D.L., 1998. High-temperature deformation of dry diabase with applications to tectonics on Venus. *Journal of Geophysical Research* 103, 975–984.
- Mancktelow, N., 1995. Nonlithostatic pressure during sediment subduction and the development and exhumation of high pressure metamorphic rocks. *Journal of Geophysical Research* 100, 571–583.

- Parsons, B.E., Sclater, J.G., 1977. An analysis of the variation of ocean floor bathymetry and heat flow with age. *Journal of Geophysical Research* 82, 803–827.
- Patriat, P., Achache, J., 1984. India–Eurasia collision chronology has implications for crustal shortening and driving mechanism of plates. *Nature* 311, 615–621.
- Pérez-Gussinyé, M., Watts, A.B., 2005. The long-term strength of Europe and its implications for plate-forming processes. *Nature* 436. doi:10.1038.
- Petrini, K., Podladchikov, Yu., 2000. Lithospheric pressure–depth relationship in compressive regions of thickened crust. *Journal of Metamorphic Geology* 18, 67–78.
- Platt, J.P., 1986. Dynamics of orogenic wedges and the uplift of high-pressure metamorphic rocks. *Geological Society of America Bulletin* 97, 1037–1053.
- Platt, J.P., 1993. Exhumation of high-pressure rocks: a review of concept and processes. *Terra Nova* 5, 119–133.
- Poliakov, A.N.B., Podladchikov, Yu., Talbot, C., 1993. Initiation of salt diapirs with frictional overburden: numerical experiments. *Tectonophysics* 228, 199–210.
- Ponziani, F., De Franco, R., Minelli, G., Biella, G., Federico, C., Piali, G., 1995. Crustal shortening and duplication of the Moho in the Northern Apennines: a view from seismic refraction data. *Tectonophysics* 252, 391–418.
- Pysklywec, R., Beaumont, C., Fullsack, P., 2000. Modeling the behavior of the continental mantle lithosphere during plate convergence. *Geology* 28, 655–658.
- Pysklywec, R.N., Beaumont, C., Fullsack, P., 2002. Lithospheric deformation during the early stages of continental collision: numerical experiments and comparison with South Island, New Zealand. *Journal of Geophysical Research* 107 (B7). doi:10.1029/2001JB000252.
- Ranalli, G., 1995. *Rheology of the Earth*, 2nd ed. Chapman and Hall, London, p. 413.
- Royden, L.H., 1993. The steady state thermal structure of eroding orogenic belts and accretionary prisms. *Journal of Geophysical Research* 98 (B3), 4487–4507.
- Sobouti, F., Arkani-Hamed, J., 2002. Thermo-mechanical modeling of subduction of continental lithosphere. *Physics of the Earth and Planetary Interiors* 131, 185–203.
- Spear, F.S., 1993. *Metamorphic Phase Equilibria and Pressure–Temperature–Time Paths*. Mineralogical Society of America, Washington, D. C., p. 799.
- Stephenson, R.A., Nakiboglu, S.M., Kelly, M.A., 1989. Effects of asthenosphere melting, regional thermoistostasy, and sediment loading on the thermomechanical subsidence of extensional sedimentary basins. In: Price, R.A. (Ed.), *Geophysical Monograph*, 48, pp. 17–27.
- Stöckhert, B., Gerya, T.V., 2005. Pre-collisional high pressure metamorphism and nappe tectonics at active continental margins: a numerical simulation. *Terra Nova* 17 (2), 102–110.
- Thompson, A.B., Jezek, J., Schulmann, K., 1997. Extrusion tectonics and rapid elevation of lower crustal metamorphic rocks in convergent orogens. *Geology* 25, 491–494.
- Toussaint, G., Burov, E., Avouac, J.-P., 2004a. Tectonic evolution of a continental collision zone: a thermo mechanical numerical model. *Tectonics* 23. doi:10.1029/2003TC001604. TC6003.
- Toussaint, G., Burov, E., Jolivet, L., 2004b. Continental plate collision: unstable versus stable slab dynamics. *Geology* 32 (1), 33–36.
- Turcotte, D.L., Schubert, G., 2002. *Geodynamics*, Second Edition. Cambridge University Press, Cambridge. 456p.
- Wenzel, F., 2002. Seismic experiments target earthquake-prone region in Romania. *Eos Transactions. American Geophysical Union*, 83, pp. 462–463.
- Wilks, K.R., Carter, N.L., 1990. Rheology of some continental lower crustal rocks. *Tectonophysics* 182, 57–77.
- Yamato, P., Agard, P., Burov, E., Le Pourhiet, L., Jolivet, L., Tiberi, C., 2007a. Burial and exhumation in a subduction wedge: mutual constraints from thermo-mechanical modelling and natural P – T – t data (sch. Lustrès, w. Alps). *Journal of Geophysical Research* 112, B07410. doi:10.1029/2006JB004441.
- Yamato, P., Burov, E., Agard, P., Le Pourhiet, L., Jolivet, L., 2007b. HP–UHP exhumation processes during continental subduction (W. Alps): when thermomechanical models reproduce P – T – t data. submitted to *Geology*.